DETERMINATION OF IMMUNE STIMULATORY PROPERTIES OF SYNTHETIC CpG OLIGODEOXYNUCLEOTIDE/CATIONIC PEPTIDE COMPLEXES

A THESIS SUBMITTED TO
THE GRADUATE SCHOOL OF NATURAL AND APPLIED SCIENCES
OF
MIDDLE EAST TECHNICAL UNIVERSITY

BY

BİLGİ GÜNGÖR

IN PARTIAL FULFILLMENT OF THE REQUIREMENTS
FOR
THE DEGREE OF MASTER OF SCIENCE
IN
BIOLOGY

SEPTEMPER 2012

Approval of the Thesis

DETERMINATION OF IMMUNE STIMULATORY PROPERTIES OF SYNTHETIC CpG OLIGODEOXYNUCLEOTIDE/CATIONIC PEPTIDE COMPLEXES

Submitted by **BİLGİ GÜNGÖR** in partial fulfillment of the requirements for the degree of **Master of Science in Biology Department, Middle East Technical University** by,

Prof. Dr. Canan Özgen _____
Dean, Graduate School of **Natural and Applied Sciences**

Prof. Dr. Musa Doğan _____
Head of Department, **Biology**

Assoc. Prof. Dr. Mayda Gürsel _____
Supervisor, **Biology Dept., METU**

Examining Committee Members:

Assoc. Prof. Dr. Can Akçalı _____
Molecular Biology and Genetics Dept., Bilkent University

Assoc. Prof. Dr. Mayda Gürsel _____
Biology Dept., METU

Assoc. Prof. Dr. Çağdaş D. Son _____
Biology Dept., METU

Assoc. Prof. Dr. Ayşen Tezcener _____
Engineering Sciences Dept., METU

Assoc. Prof. Dr. Özlen Konu _____
Molecular Biology and Genetics Dept., Bilkent University

Date: 10/09/2012

I hereby declare that all information in this document has been obtained and presented in accordance with academic rules and ethical conduct. I also declare that, as required by these rules and conduct, I have fully cited and referenced all material and results that are not original to this work.

Name, Last name : Bilgi GÜNGÖR

Signature :

ABSTRACT

DETERMINATION OF IMMUNE STIMULATORY PROPERTIES OF SYNTHETIC CpG OLIGODEOXYNUCLEOTIDE/CATIONIC PEPTIDE COMPLEXES

Güngör, Bilgi

M.Sc., Department of Biology

Supervisor: Assoc. Prof. Dr. Mayda Gürsel

September 2012, 88 pages

Synthetic CpG containing oligodeoxynucleotides (ODNs) are recognized by Toll like Receptor 9 (TLR9) and induce a strong pro-inflamatory immune response. To date, four different CpG ODN classes have been described. K-Class ODNs (also known as B-ODN) are potent B cell activators and stimulate TNFα secretion from plasmacytoid dendritic cells (pDC). D-Class ODNs (also known as A-ODNs) are the strongest stimulators of IFNα but suffer from GMP production problems through formation of undesirable multimeric structures, preventing their entry into clinical trials. In our study, conventional K-ODNs and cationic peptides TAT (+8) and LL37 (+6) were self-assembled to form nanoparticles. In contrast to free ODN, nanoparticles of sufficient stability stimulate IFNα production from both human and mouse cells. CpG ODN/peptide complexes were also shown to be good adjuvant candidates for vaccines in mouse and provide longer lasting immunity and better protection against a viral disease.

Keywords: TLR9, CpG oligodeoxynucleotides, cationic peptides, vaccine adjuvant

ÖZ

SENTETİK CpG OLİGODEOKSİNÜKLEOTİD/KATYONİK PEPTİD KOMPLEKSLERİNİN İMMÜN SİTİMÜLAN ÖZELLİKLERİNİN BELİRLENMESİ

Güngör, Bilgi

Yüksek Lisans, Biyoloji Bölümü

Tez Yöneticisi: Doç. Dr. Mayda Gürsel

Eylül 2012, 88 sayfa

CpG motifler içeren sentetik oligodeoksinükleotidler toll benzeri reseptörler tarafından tanınmakta ve güçlü bir proenflamatuar yanıtına sebep olmaktadır. Günümüzde bilinen dört çeşit CpG ODN vardır. K tipi ODN ler (B-ODN olarak da bilinirler) B lenfositleri aktif hale getirirler ve pDC hücrelerinden TNFα salınımına yol açarlar. D tipi ODN ler (A-ODN olarak da bilinirler) bilinen en güçlü IFNα uyarıcılarıdır ancak oluşturdukları istenmeyen multimerik yapılar üretimleri ile ilgili teknik sorunlar yaratmakta ve klinik uygulamalara girmelerini engellemektedir. Bu çalışma ile sıradan K-ODN lerin, TAT (+8) ve LL37 (+6) katyonik peptitler ile nanopartiküler yapılar oluşturduklarını göstermiş bulunuyoruz. Serbest ODN lerin aksine, yeterli kararlılığa sahip nanoparçacıklar hem insan hem de fare hücrelerinden IFNα salgılanmasına yol açmıştır. Ayrıca, CpG ODN/peptit komplekslerinin farelerde viral bir aşıya karşı uzun vadeli bağışıklık sağlayan başarılı aşı adjuvantı oldukları gösterilmiştir.

Anahtar Kelimeler: TLR9, CpG oligodeoksinükleotid, katyonik peptidler, aşı adjuvanı

To my Father

ACKNOWLEDGMENTS

I would like to express my deepest gratitude to my advisor, Assoc. Prof. Dr. Mayda Gürsel for excellent guidance, teaching, caring, patience, and providing me with an excellent atmosphere for doing research. She is a real scientist and perfect mentor and I fell lucky to be her student and protege.

I also want to thank the members of thesis examining committee; Assoc. Prof. Dr. Can Akçalı, Assoc. Prof. Dr. Çağdaş Devrim Son, Assoc. Prof. Dr. Ayşen Tezcaner, Assoc. Prof. Dr. Özlen Konu for evaluating this thesis; and their invaluable suggestions and comments to make the final version of this thesis better.

I would like to thank my laboratory mates Esin Alpdündar, Soner Yıldız and Mine Özcan for their help, friendship and full support. Investigation is always more charming with their existence and companionship and they are more meaningful than lab mates for me.

My sincere thanks go to Assoc. Prof. Dr. İhsan Gürsel and lab members of I.G Group for their embracement from the first day of my study. Firstly, I am grateful to Fuat Cem Yağcı, he stands by me in every step of this study, and I learned a lot of things from him. Gizem Tinçer also gives a quick guidance during my works and also writing my thesis. Thanks to Banu Bayyurt for her companionships on my experiments taking days and nights and I would like to take this occasion to thank to other members of Gürsel group Tamer Kahraman, Gözde Güçlüler, İhsan Dereli and Mehmet Şahin for their hospitability.

I would also like to thank to The Scientific and Technological Research Council of Turkey (TÜBİTAK) for their financial support to our study.

I would like to thank Institute of Foot and Mouth Disease for their FMD vaccine support in immunization studies.

I would like to thank Assoc. Prof. Dr. Kamil Can Akçalı and the staff of the animal holding facility of the Department of Molecular Biology and Genetics for their acceptance and technical support for our in vivo studies.

I would like to thank Zeynep Ergül Ülger in UNAM Confocal Microscopy Facilities for her kind assistance studies which allowed taking confocal microscopy images presented in this study.

Last but not the least; I would like to express my thanks to my family; my mother Fatma Güngör, my father Rahmi Güngör and my brothers Onur and Uğur Güngör; my brother's wife Çiğdem Güngör and my little niece Beren Güngör for believing and encouraging me throughout all my life.

TABLE OF CONTENTS

LIST OF TABLES

TABLES

LIST OF FIGURES

FIGURES

LIST OF ABBREVIATIONS

AFM	Atomic Force Microscopy
APC	Antigen presenting cell
BCIP	5-bromo-4-chloro-3’-indolyphosphate p-toluidine salt
BDCA-2	Blood dendritic cell antigen 2
bp	Base pairs
BSA	Bovine serum albumin
CCL	Chemokine (C-C motif) ligand
CD	Cluster of differentiation
cDNA	Complementary Deoxyribonucleic Acid
CpG	Unmethylated cytosine-phosphate-guaniosine motifs
CXCL	CXC-chemokine ligand
DAMP	Danger/damage associated molecular pattern
DC	Dendritic cell
DMEM	Dulbecco's Modified Eagle's Medium
DNA	Deoxyribonucleic acid
dsRNA	Double-stranded RNA
ELISA	Enzyme Linked-Immunosorbent Assay
ER	Endoplasmic reticulum
FACS	Fluorescence Activated Cell Sorting
FBS	Fetal Bovine Serum

FMD	Foot and Mouth Disease
FMDV	Foot and Mouth Disease Virus
HIV	Human Immunodeficiency Virus
hPBMC	Human peripheral blood mononuclear cell
IFN	Interferon
Ig	Immunoglobulin
IKK	Inhibitor kappa B kinase
IRF	Interferon-regulatory factor
IL	Interleukin
IP 10	Interferon gamma-induced protein 10
IRAK	IL-1 receptor-associated kinase
LBP	LPS-binding protein
LPS	Lipopolysaccharide
LRR	Leucine-rich repeat
Mal	Myeloid differentiation factor-88 adapter-like protein
MAP	Mitogen-activated protein
MAPKKK	Mitogen-activated protein kinase kinase kinase
MCP	Monocyte chemoattractant protein
Mf	Macrophage
MHC	Major histocompatibility complex
MIP	Macrophage inflammatory protein
MyD88	Myeloid differentiation factor-88
NBT	Nitro-blue tetrazolium chloride

NF-κB	Nuclear factor- kappa B
NK	Natural killer
NLR	Nucleotide-binding oligomerization domain like receptors
NOD	Nucleotide-binding oligomerization domain
ODN	Oligodeoxynucleotide
PAMP	Pathogen-associated molecular pattern
PBS	Phosphate buffered saline
PCR	Polymerase chain reaction
pDC	Plasmacytoid dendritic cell
PdI	Polydispersity index
PGN	Peptidoglycan
PI	Propidium iodine
PNPP	Para-nitrophenyl pyro phosphate
PO	Phosphodiester
poly I:C	Polyriboinosinic polyribocytidylic acid
RPMI	Roswell Park Memorial Institute
PRR	Pattern recognition receptor
RIG-I	Retinoic acid-inducible gene-I
RIP	Receptor-interacting protein
RLR	Retinoic acid-inducible gene-I like receptor
RNA	Ribonucleic acid
R848	Resiquimod
SA-AKP	Streptavidin-alkaline phospahatase

SARM	Sterile a- and armadillo-motif-containing protein
ssRNA	Single-stranded RNA
TAK1	Transforming growth factor β activated kinase-1
Th1	T helper type 1
Th2	T helper type 2
TIR	Toll–interleukin 1 receptor
TLR	Toll-like receptor
TNF	Tumor necrosis factor
TRAF	TNF-associated factor
TRAM	TRIF-related adaptor molecules
TRIF	TIR domain containing adaptor inducing IFN-β

CHAPTER 1

INTRODUCTION

1.1. Immune System

Over the course of evolution, from bacteria to humans all organisms have evolved a number of strategies to counteract pathogenic invaders. In higher organisms, the combination of a variety of defense mechanisms is collectively called as the immune system. All immune systems require discriminating nonself foreign agents from their own components and eliminating the nonself outsiders or altered-self cells such as, those infected by viruses or transformed as a result of cancer (Sun, 2008). The immune system in humans and other mammals is more complex than the one present in invertebrates since there are two interrelated types of immunity in mammals: the innate immune system, which is more instantaneous and evolutionarily more ancient and the adaptive immune system, which is highly specific and is activated in a delayed fashion (Litman, 2005). These two systems have different working principles; innate immune system recognizes invaders by a small number of germ line encoded receptors whereas the receptors of adaptive immune system are randomly generated, clonally expressed and highly specific (Palm, 2009).

Physical barriers of the body, including the skin and the mucosal epithelial layers, constitute the first line of defense against pathogen entry (Lievin-Le Moal, 2006). Pathogens that have succeeded to penetrate the physical barriers are encountered by the innate arm of the immune system. Innate immune cells recognize the “danger signals” of pathogenic invaders and produce large amounts of proinflammatory molecules, aiding in removal of the invader and preventing its spread to other tissues. Dendritic cells (DCs), also called as the professional antigen presenting cells (APCs), belong to the innate immune system and are pivotal in alerting the adaptive immune

system to the presence of pathogens (Tel, 2012). DCs phagocytose the pathogen, process the antigens into peptides and present these peptides in association with major histocompatibility complex (MHC) class I and II molecules to $CD8^+$ and $CD4^+$ T cells, respectively (Cervantes-Barragan, 2012).Furthermore, pathogen recognition by DCs leads to de-novo surface expression of co-stimulatory molecules (CD80 and CD86) that are essential for priming of naïve T cells in the lymph nodes. Accordingly, the innate immune system is vital in the induction of the adaptive immunity and both systems are highly interconnected (Palm, 2009).

The focus of this study is to develop an immunostimulatory agent particularly suited to combat viral infections and capable of providing long-lasting immunity when used in vaccines as an adjuvant.

1.2. Innate Immune System

The innate immune system is the first line of host defense and consists of many different units and subsystems. The first barrier that pathogens encounter is the skin and the mucosal epithelia. The epithelial cells and keratinocytes are specialized cells capable of producing antimicrobial peptides which restrain the pathogens (Hiroshima, 2011). Thus, the mucosal epithelia functions as a chemical barrier as well (Medzhitov, 2007). Another key element of the innate immune system is inflammation, a process that prevents the spread of infection. This process is initiated by tissue resident specialized innate immune cells such as macrophages and dendritic cells that express a variety of pattern recognition receptors (PRRs). These receptors recognize pathogen-associated molecular patterns (PAMPs). PAMPs are shared by pathogens but are not found in/on host cells and because these patterns are vitally important for survival of the pathogens, they are conserved among microorganisms. However, host-derived factors such as heat shock proteins or ATP are also released from injured cells and can contribute to inflammation at the site of damage. Similar

to PAMPs, these danger/damage associated molecular patterns (DAMPs) are also recognized by PRRs (Seong and Matzinger, 2004). Recognition of pathogens or injured cell remnants initiates the release of inflammatory mediators and recruits phagocytes like neutrophils, which further contribute to immune activation. The inflammatory response is mainly mediated by cytokines and chemokines secreted by activated cells (please see Table 1.1. and Table 1.2.). The innate immune system has specialized cells other than macrophages, dendritic cells and neutrophils. For instance, natural killer cells (NK cells) detect virally infected host cells and clear them (Shereck, 2007). Eosinophils, basophils and mast cells mainly have a role in protection from multicellular parasites (Stone, 2010). One of the subsystems of the innate immunity is the complement system that helps to mark the pathogen by opsonization or cause cytolysis of the pathogen via pore formation in their membranes (Degn, 2007). The complement system is composed of several small proteins. Following the activation of the complement cascade, these proteins are sequentially cleaved and activated, culminating in the formation of the membrane attack complex.

One of the most important functions of the innate immune system is the activation of the adaptive immune response through the process of antigen presentation (Watts, 2010). Tissue resident immature dendritic cells express PRR and accessory receptors that collectively contribute to pathogen recognition, initiating DC maturation. Mature DCs lose their phagocytic ability and migrate to the closest draining lymph nodes where antigen presentation to naive T cells takes place. Furthermore, the nature of the recognized pathogen (i.e which PRRs are activated) determines the type of the adaptive immune response generated. For example, recognition of intracellular bacteria by DCs triggers the release of interleukin-12 and T cells that are primed by these DCs differentiate into T helper type 1 (Th1) cells, which are particularly effective in combating intracellular pathogens (Kis-Toth, 2011). Therefore, DCs serve as a link between innate and adaptive immunity, capable of determining the

type of adaptive immunity that is most effective against a specific pathogen (Walport, 2008).

Table 1.1 Cytokines affect behavior of target cells (Adapted from Murphy, 2008).

Cytokine	**Produced by**	**Function**
IL-1β	Mf, keratinocytes	Fever, induction of acute-phase protein secretion, T cell and Mf activation
TNFα	Mf, DC, NK and T cells	Local inflammation and endothelial activation
IL6	Mf, DC	Fever, T and B cell growth and differentiation
IL-12	Mf, DC	Activation of NK cells, induction of CD4 T-cells to differentiate into T_H1
IL-15	Many non-T cells	CD8 memory T cell survival, stimulation of NK and T cell growth
IL-18	Activated Mf	Induction of IFNγ secretion via NK and T cells, favors T_H1 immunity
IFNα	DC	Anti-viral immunity, induction of MHC I expression
IFNγ	T cells, NK cells	Suppression of T_H2 immunity, Mf activation, increased expression of antigen processing components

Table 1.2 Chemokines recruit target cells to sites of infection. (Adapted from Murphy, 2008).

Chemokines	**Produced by**	**Attracted cells**	**Major effect**
CXCL8 (IL-8)	Monocytes, Mf, DC	Neutrophils, naïve T cells	Mobilization, activation and degranulation of neutrophils
CCL3 (MIP-1α)	Monocytes, T and Mast cells, fibroblasts	Monocyte, NK, T cells basophil, DC	Promotes T_H1, antiviral defense, competes with HIV-1
CCL4 (MIP-1β)	Monocytes, Mf, Neutrophils, endothelium	Monocyte, NK, T, DC	Competes with HIV-1
CCL2 (MCP-1)	Monocyte, Mf, fibroblast, keratinocyte	Monocyte, NK, T, DC basophil	Promotes T_H2, activate Mf, histamine release from basophils
CXCL10 (IP10)	T, fibroblast, endothelial,monocyte, keratinocyte	Resting T cells, NK, monocytes	Promotes T_H1, antiangiogenic, immunostimulant

1.2.1. Pattern Recognition Receptors (PRRs)

Pattern recognition receptors are germline-encoded nonclonal receptors and detect PAMPs, and DAMPs to trigger a signaling cascade culminating in a proinflammatory responses. PAMPs are vital for the survival of the pathogens and so they were conserved through evolution. These molecules are invariant among microorganisms. Lipopolysaccharide (LPS), peptidoglycan, lipoteichoic acid like cell-wall components of bacteria; β-glucan of fungal cell wall; DNA containing unmethylated cytosine-phosphateguanine (CpG) motif in bacterial genome; viral double stranded RNA (dsRNA), and single stranded DNA (ssDNA) are considered as classical PAMPs (Akira, 2006). Several different receptors participate in pattern recognition and are equipped with pathogen recognizing protein domains such as the C-type lectin domain (Hollmig, 2009), scavenger receptor cysteine-rich domain and leucine-rich repeat (LRR) domain. PRRs can be expressed on the surface of immune or non-immune cells, present in the cytoplasm, in endosomes or found in the body fluids as secreted proteins. The secreted PRRs contribute to opsonization of pathogens and initiate complement activation. PRRs enhance uptake of pathogens by phagocytes and dendritic cells and initiate signaling pathways that trigger the release of inflammatory cytokines, chemokines or antimicrobial peptides (Medzhitov, 2000). There are three main PRR families: 1. Toll-like receptors (TLRs), 2.Nucleotide-binding oligomerization domain (NOD)-like receptors (NLRs) and 3. The retinoic acid-inducible gene-I (RIG-I)-like receptors (RLRs).

1.2.1.1 Toll Like Receptors (TLRs)

The first identified and most well characterized PRR group was toll like receptors (TLRs). Toll was originally identified as an embryonic protein crucial during the Drosophila development (Valanne, 2011). Later, it was found to be important in mediating an antifungal response in files. To date, 10 human and 12 mouse TLRs have been found (Kawai, 2010). TLR1-TLR9 are conserved between human and

mice. TLR10 is not functional in mice and TLR11, TLR12 and TLR13 are lost in human genomes (Kawai, 2009). TLRs are type I transmembrane proteins and consist of three domains: 1. the ectodomain contains leucine-rich repeats that mediate the recognition of PAMPs; 2.the transmembrane domain; 3. the intracellular Toll–interleukin 1 (IL-1) receptor (TIR) domain that is required for downstream signal transduction. TLRs are capable of recognizing a variety of PAMPs such as lipids, lipoproteins, proteins and nucleic acids derived from a wide range of microbes such as bacteria, viruses, protozoa and fungi. Table 1.3 summarizes the TLRs and their ligands.

Table 1.3 Toll-like receptors (TLRs) and some of their important ligands (Adapted from Trinchieri, 2007).

Pathogen	Toll-like receptor (TLR)	TLR ligand
Mycobacterium tuberculosis	TLR2	Lipoarabinomannan
	TLR4	Phosphatidylinositol mannosides
	TLR9	DNA
Salmonella typhimurium	TLR2	Bacterial lipoprotein
	TLR4	Lipopolysaccharide
	TLR5	Flagellin
Neisseria meningitidis	TLR2	Porin
	TLR4	Lipopolysaccharide
	TLR9	DNA
Haemophilus influenzae	TLR2	Lipoprotein
	TLR4	Lipopolysaccharide
Candida albicans	TLR2	Phospholipomannan
	TLR4	Mannan
	TLR9	DNA
Murine cytomegalovirus	TLR2	Viral protein
	TLR3	Double-stranded RNA
	TLR9	DNA
Herpes simplex virus	TLR2	Viral protein
	TLR3	Double-stranded RNA
	TLR9	DNA
Influenza virus	TLR7, TLR8	Single-stranded RNA
	TLR3	Double-stranded RNA
	TLR4	Not determined
Respiratory syncytial virus	TLR3	Double-stranded RNA
	TLR4	Envelope F protein
Trypanosoma cruzi	TLR2	Glycosylphosphatidylinositol anchor
	TLR4	Glycoinositolphospholipid-ceramides
	TLR9	DNA
Toxoplasma gondii	TLR2	Glycosylphosphatidylinositol anchor?
	TLR11	Profilin

Toll like receptors can be found in different cellular compartments. They are expressed on the cell surface or in intracellular vesicles like the endosomes and in ER. The cellular localization of TLRs determines the ligand accessibility, the maintenance of tolerance to self molecules such as nucleic acids and downstream signal transduction. (Kumar, 2009). Figure 1.1 presents cellular localization of TLRs.

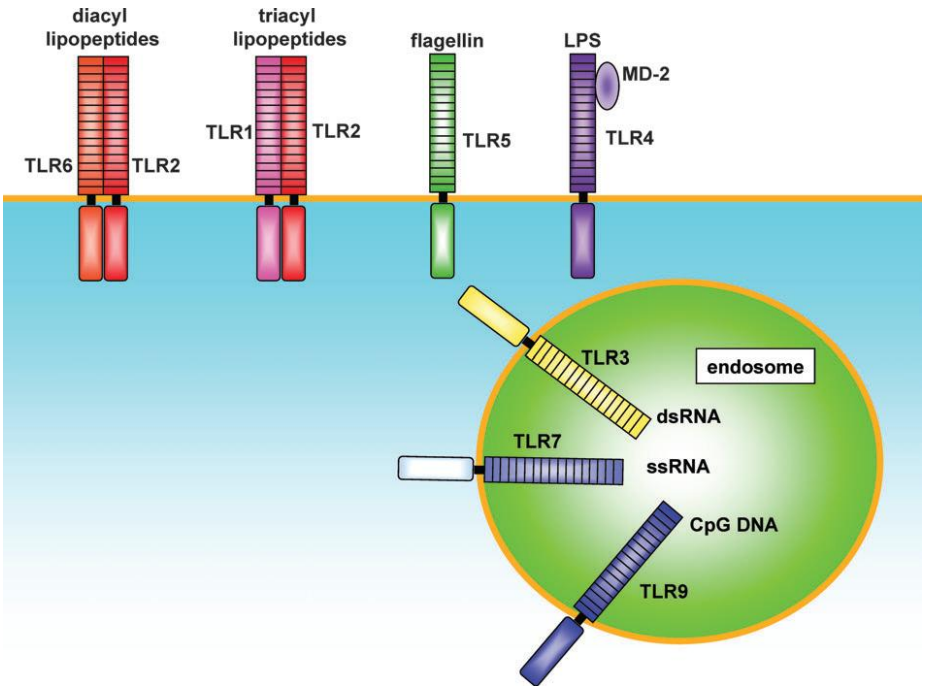

Figure 1.1 Cellular localization of TLRs (Adapted from Takeda and Akira, 2005)

1.2.1.1.1. Extracellular TLRs

TLR1, TLR2, TLR4, TLR5, TLR6 and TLR11 (only in mice) are expressed on the cell surface and they mainly recognize microbial membrane components (Kaisho, 2001). TLR2 can recognize a wide range of PAMPs. For instance, they recognize lipopeptides from bacteria, peptidoglycan and lipoteichoic acid from Gram-positive

bacteria, zymosan from fungi, lipoarabinomannan from mycobacteria or the hemagglutinin protein from measles virus. TLR2 generally forms heterodimers with TLR1 or TLR6. The TLR2-TLR1 heterodimer recognizes triacylated lipopeptides from Gram-negative bacteria and mycoplasma, while the TLR2-TLR6 heterodimer recognizes diacylated lipopeptides from Grampositive bacteria and mycoplasma. TLR2 ligands generally trigger the production of pro-inflammatory cytokines (Kawai, 2010).

TLR4 mainly recognizes bacterial lipopolysaccharide (LPS), a component of the outer membrane of Gram-negative bacteria (Lu, 2008). TLR4 forms a complex with MD2 on the cell surface, and together they serve as the main LPS-binding component. TLR4 needs additional proteins for LPS binding such as LPS-binding protein (LBP) which is a soluble plasma protein and binds LPS. CD14 is glycosylphosphatidylinositol-linked, leucine-rich repeat–containing protein is also involved in LPS binding via binding to LBP and delivering the LPS-LBP to the TLR4-MD2 complex. Two copies of the TLR4-MD2-LPS complex initiates signal transduction by recruiting intracellular adaptor molecules. Other than LPS, TLR4 can also recognize respiratory syncytial virus fusion proteins, mouse mammary tumor virus envelope proteins, and *Streptococcus pneumoniae* pneumolysin (Luxameechanporn, 2005).

TLR5 recognizes flagellin protein which is a component of bacterial flagella (Yoon, 2012). Flagellin is a protein different from other PAMPs and unlike host proteins it is not subjected to any posttranslational modifications. The highly conserved - carboxy-termini of flagellin is essential for bacterial mobility. TLR5 is predominantly expressed on the basolateral side of the intestinal epithelium, a major entry point for most pathogenic bacteria (Medzhitov, 2001).

TLR11 is a relative of TLR5 and functional in mice but is lost from the human genome. TLR11 is highly expressed in the kidney and bladder of mice and recognizes uropathogenic bacterial components. TLR11 also recognizes the profilin-like molecule derived from *Toxoplasma gondii* and generates a powerful NF-κB-dependent inflammatory response and subsequent IL12 production (Kucera, 2010).

1.2.1.1.2. Intracellular TLRs

Intracellular TLRs are TLR3, TLR7, TLR8, and TLR9. These receptors are specialized to sense nucleic acids and are localized within intracellular vesicles (endosomes, lysosomes, and endolysosomes) and in the endoplasmic reticulum (ER). The intracellular localization permits for detection of pathogen-derived nucleic acids following their uptake and triggers mainly an anti-viral innate immune response by including type I IFNs and inflammatory cytokines (Blasius, 2010). TLRs, residing in the ER, are delivered to the endosomes where they encounter the PAMPs. The N-terminal region of the TLRs are then processed by multiple lysosomal proteases, including cathepsins and asparagines endopeptidase in the endosomes and become functional receptors (Blasius and Beutler, 2010).

TLR3 recognizes dsRNA, a common intermediate of viral replication (Botos, 2009). It is known that both positive stranded RNA viruses and DNA viruses produce detectable dsRNA transcripts, whereas negative strand RNA viruses do not produce such transcripts. Therefore, TLR3 plays a role in the response to dsRNA viruses, as well as DNA and positive stranded RNA viruses but has no role in protection against negative stranded RNA viruses (Weber, 2006). As a TLR3 ligand, a synthetic analog of viral dsRNA, polyriboinosinic polyribocytidylic acid (poly I:C) has been used in experimental studies to mimic viral infection (Schröder, 2005).

TLR 7 recognizes ssRNA, imidazoquinoline derivatives such as resiquimod (R848) and imiquimod, imidazoquinoline, and guanine analogs such as loxoribine (Diebold,

2004; Heil, 2004). TLR8 functions to detect ssRNA in humans but is reduntant in mice (Jurk, 2002).

TLR9 recognizes bacterial and viral DNA via the presence of unmethylated CpG motifs (Klinmann and Kreig, 1995). The mammalian DNA has 20 X lower frequency of CpG motifs compared to prokaryotes and the CpG motifs are mostly methylated. Therefore, mammalian DNA is usually not a ligand of TLR9 (Hemmi, 2000).

1.2.1.2. TLR signaling pathways

TLRs recognize components of pathogens and mediate a protective immune response. TLRs share common signaling pathways, but the outcome of the resultant inflammatory response varies between TLR agonists (Bagchi, 2007). For instance, activation of TLR3 and TLR4 signaling pathways results in production of type I IFNs. Similarly, signaling through TLR7, TLR8 and TLR9 also stimulate induction of type I IFNs but involve other signaling components (Ito *et al.* 2002). All TLRs, except for TLR3, possess a conserved cytoplasmic proline residue in their TIR domains that critically contribute to signaling (Kawai, 2007). TLR dimerisation recruits the TIR–TIR interface and signaling is initiated by the TIR adaptors. There are five TIR adaptors: myeloid differentiation factor-88 (MyD88), MyD88 adapter-like protein (Mal), TIR domain- containing adaptor protein inducing IFNβ (TRIF), TRIF-related adaptor molecule (TRAM) and sterile a- and armadillo-motif-containing protein (SARM) (Kenny, 2008). There are two different TLR signaling pathways: all TLRs except for TLR3 use the adaptor MyD88, whereas TLR3 signaling is MyD88 independent but TRIF dependent. TL4 can signal through both pathways (Figure 1.2).

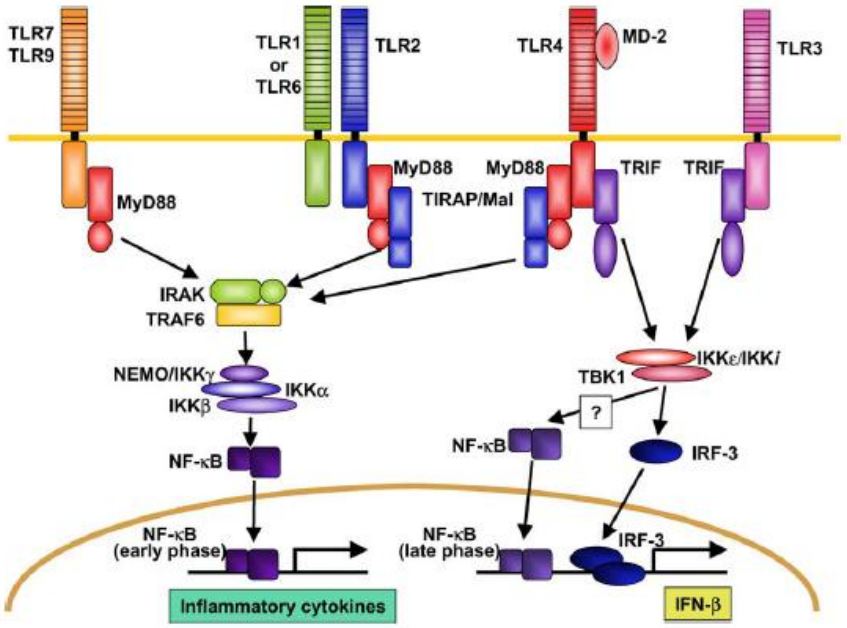

Figure 1.2 TLRs Signaling Pathways: The Figure summarizes the MyD88 Dependent and MyD88 Independent TRIF-dependent signaling components (Adapted from Takeda, 2004)

1.2.1.2.1. MyD88 Dependent Pathway

Following ligand binding, TLR dimerization and MyD88 recruitment, kinases that belong to the IRAK family, including IRAK1, IRAK2, IRAK4 and IRAK-M are recruited and activated. IRAK4 is the main kinase that is essential for the activation of the MyD88-dependent pathway. Once phosphorylated, IRAKs dissociate from MyD88 and interact with TRAF6, an E3 ligase which in turn forms a complex with Ubc13 and Uev1A. This complex assists the synthesis of lysine 63-linked polyubiquitin chains and activates TAK1, a MAP kinase kinase kinase (MAPKKK) (Chen, 2005). TAK1, in combination with TAB1, TAB2 and TAB3, activates two downstream pathways involving the IKK complex and the MAPK family. Once activated, the IKK complex induces phosphorylation and subsequent degradation of IkB, which leads to nuclear translocation of the transcription factor NF-kB (Takeda,

2004). MyD88 is crucial for the inflammatory cytokine production through all TLRs. MyD88-deficient mice do not show production of inflammatory cytokines such as TNF-α and IL-12p40 in response to all TLR ligands except for TLR3 and TLR4 (Klinman, 2004).

1.2.1.2.2. MyD88-independent-TRIF dependent pathway

MyD88-deficient mice are responsive to TLR3 and TLR4 ligands and use a different adaptor for signaling (TRIF) (Yamamato, 2003; Kawai, 2007). Stimulation through TLR3 and TLR4 cause overexpression of TRIF which in turn activates IRF3 and NFκB (Hoebe, 2003). The N-terminal and the C-terminal sites of TRIF have different functions. Type I IFN and NF-κB promoters are activated by the N-terminal region of TRIF while NF-κB but not the type I IFN promoter is activated by the C-terminal region (Sharma, 2003). The N-terminal leads to phosphorylation of the serine/threonine clusters present in the C-terminal region of IRF3 which forms a dimer and translocates from cytoplasm to the nucleus to induce expression of target genes, including IFNβ (Fitzgerald, 2003).

In brief, all TLRs activate NF-kB through the MyD88- or TRIF-dependent pathways. MyD88 activates NFkB via the IRAKs–TRAF6–TAK1–IKKα/β pathway. TRIF activates NF-kB through the RIP1/TRAF6–TAK1–IKKα/β pathway. The activation of NFkB is crucial in the production of proinflammatory cytokines during the innate immune responses and contributes to consequent development of an adaptive immune response (Newton, 2012).

1.3. Therapeutic Potential of TLR Ligands with an Emphasis on TLR9

1.3.1. CpG ODNs

TLR9 recognizes the unmethylated CpG motifs present at high frequency in bacterial DNA but rare in mammalian DNA, due to CG suppression and CG methylation in the latter (Krieg, 1995). Synthetic oligodeoxynucleotides (ODN) expressing unmethylated CpG motifs duplicate the ability of bacterial DNA to stimulate the innate immune system via TLR9. CpG-ODNs directly activate dendritic cells (DCs) and B cells and contribute to natural killer (NK) cell and T cell activation indirectly via the CpG-ODN-induced cytokines and chemokines, favoring a Th1-type response (Figure1.3; Hanagata, 2012). Therefore, synthetic CpG ODNs are designed and widely used as immunoprotective agents and vaccine adjuvants in various preclinical and clinical studies such as infectious diseases, cancer therapies, and allergies (Liu, 2011).

The immune stimulatory effects of CpG-ODNs diversify depending on the number of CpG motifs, backbone modification, length, flanking sequence, and formation of secondary and tertiary structures (Kreig, 2006). Since unmodified ODNs have a phosphodiester backbone prone to nuclease attack in serum (i.e, DNase), phosphorothioate backbone modifications were introduced to enhance resistance (Heeg, 2008). The minimum ODN length required for immune stimulation was found to be 8 bp. Methylation of the cytosine in CpG or its conversion to a GpC, leads to loss of immune stimulatory activity and these ODNs are used as controls in immune stimulation studies (Wagner, 2008).

The sequences that flank the CpG motifs are important in determining the stimulatory properties of the ODN. In mouse, the optimum stimulatory central hexameric sequence is PuPuCpGPyPy, whereas in humans this is a PuPyCpGPuPy (Pu: purine; Py: pyrimidine) (Krieg A, 1995; Verthelyi D, 2001). To date, based on

their immune stimulatory effects, four different classes of synthetic CpG ODNs have been defined: i) A or D-type CpG, ii) B or K-type CpG, iii) C-type CpG and iv) P-type CpG ODNs. Properties of each class are discussed below (Vollmer, 2006) and their characteristic features are presented in Table 1.4 and Figure 1.4.

1.3.1.1. A (D type) CpG ODNs

'D' class ODNs (also known as A class) possess a mixed backbone (phosphodiester/ phosphorothiote) and have G (guanosine) runs with PS linkages at the 5′ and 3′ ends. These G runs are on either side of a single CpG motif embedded within a palindromic region of a phosphodiester (PO) backbone (Figure 1.3) (Endres, 2001; Vollmer, 2009). The minimum length of an active D-ODN is 18 bp. (Verthelyi D, 2001). This palindromic sequence causes a duplex formation and the four Gs within the poly(G) sequences at the end of these duplexes combine with one another via Hoogsteen base pairing to form a G-tetrad structure. Consequently, D type ODNs form G-quadruplexes and higher order structures that can be globular (~50nm size), linear (~100nm size) or two forked (Figure1.3) (Klein, 2010). These structural features generate a more stable ODN and increase its cellular uptake efficiency since poly(G) binds to scavenger receptors on the cell surface. The most important characteristic of this ODN class is its ability to trigger IFNα release from plasmacytoid dendritic cells (pDCs) (Gürsel M., 2002; Gursel M 2006).

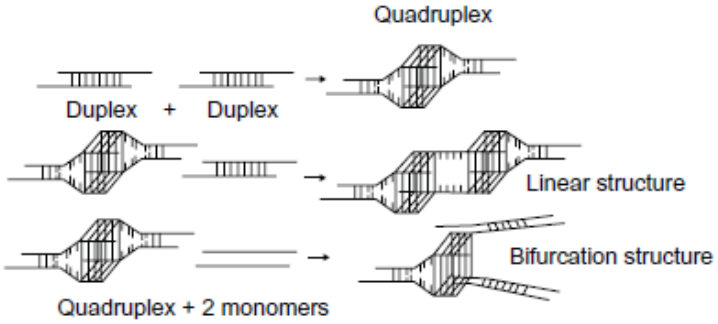

Figure 1.3 Model of higher-order structures formed by D class ODNs. The hydrogen bonds between 4 G residues are Hoogsteen base pairs, forming G-quadruplexes (adopted from Hanagata, 2012)

They also indirectly induce IFN-γ and IP-10 from PBMC and contribute to NK cell-mediated cytolytic activity (Vollmer, 2009). They induce the expression of co-stimulatory molecules such as CD80, CD86 and HLA-DR on pDC and B cells moderately (Krug, 2001). D-ODN stimulates monocytes to mature into CD83+/CD86+ dendritic cells in an IFN-α-dependent manner (Gursel M, 2002b). Although strong IFN-alpha and IFN-beta stimulators, D-ODN are weak in triggering pDC maturation or B cell proliferation. In mouse splenocytes D-type ODN stimulates moderate levels of IL-6, IL-12 and high levels of IFN-γ (Vollmer, 2004).

In short, D-ODNs cause a Th-1 dominated immune response and are potent IFNα inducers but suffer from pharmaceutical production problems due to unpredictable higher order structure formation that prevents their entry into clinical trials (Wang, 2008).

1.3.1.2. B (K type) CpG ODNs

K Class ODNs (also known as B class) have a complete phosphorothioate backbone and multiple CpG motifs (Vollmer, 2004 ; Hartmann, 2003). In contrast to D-ODN,

K-ODNs lack polyG tails and remain as single stranded linear sequences (Costa, 2004) (Verthelyi D, 2001).

K-ODNs are potent activators of $CD19^+$ B cells (Gursel M, 2002a), triggering IL-6 and IgM secretion and proliferation (Jung, 2002). K ODNs can induce pDC maturation and trigger proinflammatory cytokines secretion from these cells (Marshall, 2003; Gursel, 2002; 2006). Unlike D-ODNs, they fail to stimulate IFNα production from pDCs but trigger TNFα secretion from them (Gray, 2007; Gursel 2006). They induce low amounts of IFNγ and IP10 secretion from human PBMCs but are more potent in mice. Spleen cells also secrete very high amounts of IL-6 and IL-12 in response to K-type ODNs (Blackwell, 2003), contributing to Th1 dominant responses.

1.3.1.3. C-type CpG ODNs

The C-ODN combines the characteristics of the A- and B-Classes. They induce strong B-cell activation similar to B-ODN together with IFNα secretion similar to D-Class ODN (Jurk, 2004), albeit at very low amounts. It has an entire PS backbone with 5' CpG sequences ('TCGTCG motif') and a 12-16 bp palindromic sequence at its 3' end (Vollmer, 2004). This GC-rich palindromic sequence is linked by a T spacer to the stimulatory hexameric CpG motif positioned at or near the 5′. The physical linkage between these two domains is vital for the immune activity. (Krieg AM, 2006) (Hartmann, 2003; Vollmer, 2004). The C-ODN was specifically designed to bypass the manufacturing problems experienced with the D-ODN so that they could be included in clinical studies. Unfortunately, they are still weak IFNα inducers and fail to replace the activity of D-ODN.

1.3.1.4. P Type CpG ODNs

The more recent P class ODNs were a result of another attempt to replace D-ODN and were also designed to stimulate IFNα secretion by pDCs. P-Class contains two palindromic sequences that form concatamers in high-salt buffers (Samulowitz, Weber, Weeratna, Uhlmann, Noll, Krieg, Vollmer). This novel class of immune-stimulatory CpG oligodeoxynucleotides unifies high potency in type I interferon induction with preferred structural properties. (Samulowitz, 2010). Although this ODN class can trigger higher levels of IFNα than the C-ODN, they are still not as potent as D-ODN and their dependence on "high-salt buffers" to form the IFNα stimulating higher order structures makes them unpredictable for in vivo applications.

Table 1.4 Classes and characteristics of cytosine-phosphate-guanosine (CpG) oligodeoxynucleotides (ODNs) (Adapted from Hanagata, 2012).

	Class A (type D)	Class B (type K)	Class C	Class P
ODN structure	Central phosphodiester region containing one or more CpG motifs in a palindrome and 5′ and/or 3′ ends consisting of poly(G) motifs with phosphorothioate backbone	Completely phosphorothioate backbone	One or more 5′ CpG motif(s) and a 3′ palindrome	Two palindromes consisting of phosphorothioate backbone
Examples	ODN2216 (for human) ODN2336 (for human) ODN1585 (for mouse)	ODN2006 (also know as PF-3512676 and CpG7909, for human) ODN1668 (for mouse) ODN1826 (for mouse)	ODN2395 (for human and mouse) ODN M362 (for human and mouse)	ODN21798
Mainly stimulated cell types	pDCs	B cells	pDCs and B cells	pDCs
Actions	Innate immune responses: IFN-α, TNFα, and IL-12 secretion Adaptive immune responses: IL-12 and IP10 secretion	Innate immune responses: IL-6, IL-10, and IL-12 secretion Adaptive immune responses: antibody production; IL-6 and IL-12 secretion	Intermediate between the A and B classes	Potency for IFN-α secretion is higher than that of CpG ODN in class C

Figure 1.4 Examples of CpG ODN sequences from each class. Palindromic sequences are underlined; black and red hyphens indicate phosphodiester and phosphorothioate bonds, respectively (Adapted from Hanagata, 2012).

1.3.3 Signaling Through TLR9

Although both K and D type CpG ODNs are recognized by TLR9, they result in differential immune activation; the K-ODN stimulates TNFα secretion from pDCs with very little or no induction of IFNα, whereas 'D' class ODNs trigger high levels of IFNα but no TNFα from the same cells. D-ODN but not K-ODN were shown to bind to a scavenger receptor known as CXCL16 expressed on pDCs (Gursel, 2006). This process sequesters D-ODN in early endosomes for a longer period of time, while K-ODN immediately localizes to lysosomal vesicles. Recognition of K-ODN in late endosomes leads to the colocalization of MyD88 and IRF5 with TLR9 and induce TNFα secretion (Asselin, 2005). On the other hand, D-ODN recognition by TLR9 in early endosomes of pDCs leads to the colocalization of MyD88 and interferon regulatory factor (IRF)-7 with TLR9 and following downstream signaling, induces IFNα production. (Honda, 2005). Prolonged signaling allows continuous activation of the positive feedback system and phosphorylation of de novo

synthesized IRF7 to induce robust type I IFN production (Asselin, 2005; Honda, 2006) (Figure 1.5).

In conclusion, formation of higher order structures organizes compartmental retention and intracellular distribution. The D-ODN localizes to a different endolysosomal compartment than the K-ODN (Cao, 2007). Therefore, D-ODN triggers IRF-7- mediated intracellular signaling pathways from early endosomes and stimulate strong IFNα production, whereas the K-ODN mainly stimulates NFκB-mediated signaling from late endosomes and initiates proinflammatory cytokines such as TNFα, IL-6 and IL-12 production and strong B cell activation (Kumagai, 2008).

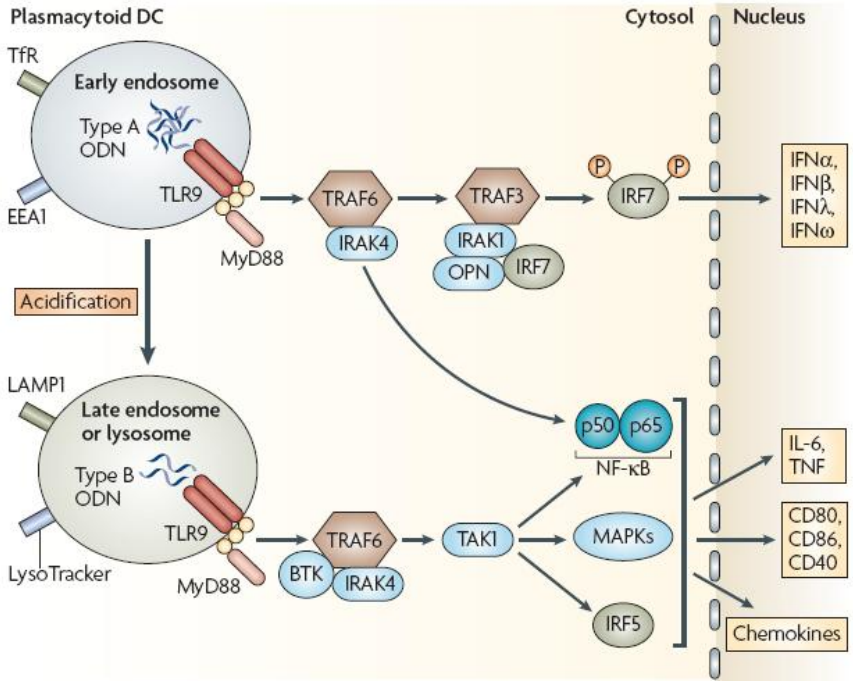

Figure 1.5 Mechanism of differential immune activation induced by D-Class and K-Class ODN (Gilliet. 2008).

1.3.4 CpG ODNs as Therapeutics

CpG ODNs are potent stimulators of innate and adaptive immune responses (Figure 1.6). Murine models indicate that the innate immune response elicited by CpG ODN can be harnessed to help eliminate cancers, prevent allergic reactions and boost the immunogenicity of vaccines (as reviewed in Klinman, 2006; Klinman, 2009; Steinhagen, 2011; Bode et al, 2011). TLR9 is expressed by B lymphocytes, all DC types and macrophages in mice, but its expression is restricted to B cells and pDCs in humans (Hemmi, 2000; Takeshita, 2001).

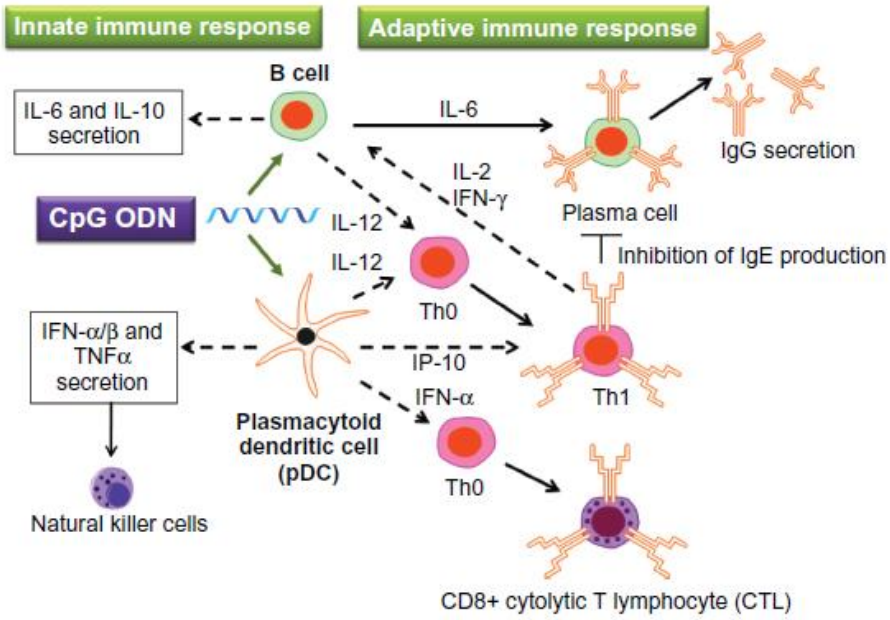

Figure 1.6 Innate and adaptive immune responses stimulated by CpG ODNs (Adapted from Hanagata, 2012)

This restricted expression pattern limits the success of conventional CpG ODN (K type) in humans, necessitating the use of other ODN classes that induce more potent cytokines, such as IFNα. However, as mentioned above, D-ODN can only enter into clinical trials if they are modified to maintain their structural integrity, for example

by incorporation into virus like particles (Senti et al., 2009). A facile strategy is to convert a K-type ODN into a nanoparticulate form via complexation with poly cationic peptides. Since the ODN is negatively charged, interaction with cationic molecules is favored, simplifying the production as a therapeutic (Charalambos, 2009). Recent studies showed that CpG ODN complexed with an antimicrobial peptide LL37 triggers enhanced immune response from B cells and pDCs (Lande, 2007; Hurdato 2010). LL-37 is native peptide derived from the amino acids [aa] 104 to 140 of the human cathelicidin antimicrobial peptide (Cristina, 2005). Induction of LL-37 expression from epithelial cells during bacterial infections leads to efficient lysis of the invading microbes. LL37 peptide can form complexes with extracellular DNA and enhance their cellular uptake (Sandgren, 2004). Investigations about nano-sized complexes of CpG ODN and LL37 indicated that LL37 complexation changes the cellular distribution of ODN to stimulate pathways for IFNα production. The anti-tumor effects of CpG ODN/LL37 complex was also studied in mouse (Chuang, 2009). Unfortunately, cytotoxic effects of LL37, especially on mammalian red blood cells, are a concern, limiting the clinical potential of the peptide. On the other hand, the shortest active part of the LL37 peptide, KR12 was reported to be safer and nontoxic for mammalian cells, but its potential use together with CpG ODNs was not explored before (Wang, 2009). One other cationic peptide, TAT (HIV derived peptide) was complexed with K type CpG ODN and was shown to induce cytotoxic T cells when used as a vaccine adjuvant. However, how these complexes activated the immune system was not studied, requiring further investigations (Partidos, 2009).

1.4 Foot and Mouth Disease Vaccine

1.4.1 Foot and Mouth Disease (FMD)

Foot-and-mouth disease (FMD) is a viral disease affecting cloven hoofed animals, such as cattle, pigs, deer, goats and sheep. The disease is characterized by fever, lameness and vesicular lesions on the feet, tongue, snout and teats, with high morbidity but low mortality (Segundo, 2011). It is a severe and highly contagious disease with frequent outbreaks around the world (Zhang, 2011). FMD is one of the most important economically devastating animal diseases since it causes a significant decrease in animals' weight and milk output and thus reduces animals' commercial value (Mort, 2005). In the past decade FMD arouse global concern as a potential bio-terror danger since several new outbreaks in previously FMD-free countries (Rodriguez, 2009) were observed. Thus, it is essential to prevent, control and eliminate FMD through successful vaccination campaigns.

1.4.2 Foot and Mouth Disease Virus (FMDV)

FMD virus (FMDV), the causative agent of the foot and mouth disease, is a member of the genus *Aphthovirus* which belongs to the *Picornaviridae* family. It is an RNA virus containing a single strand of RNA. The size of the virus is 25-30 nm and it has an icosahedral capsid made of protein, without envelope (Carrillo, 2005). It causes infection through the respiratory tract following contact or inhalation of airborne FMD (Alves, 2009). Seven serotypes of the virus has been identified so far: A, O, C, Asia1, Southern African Territories (SAT) 1, SAT2 and SAT3 . Distribution of these serotypes across the world changes regionally. The most common type is serotype O, distributed throughout Middle East, Asia and Southern America (Domenech, 2010) (Table 1.5).

Table 1.5 Serotypes and regional distribution of FMDV (Adapted from Zhang, 2011).

Area	Main serotypes in FMDV distribution areas						
	Type O	Type A	Type C	Type Asia I	SAT-1	SAT-2	SAT-3
China	+	+	-	+	-	-	-
Southeast Asia	+	+	-	+	-	-	-
Africa	+	-	-	-	+	+	+
Middle East	+	+	+	+	-	-	-
United Kingdom	+	-	-	-	-	-	-
South America	+	+	+	-	-	-	-

"+" means positive, and "-" means negative.

The distinctive feature of the FMDV infection is the vesicular lesions in epithelia of the mouth and coronary bands of the hoof (Grubman, 2004). Following exposure, FMDV initially replicates in the pharynx. The virus invades the blood stream within 24–48 hours and, shortly after, lesions appear in the mouth and feet (Pacheco, 2008). The virus replicates to very high titers (>8 log 10 infectious units per ml) at the lesion site even though viremia disappears after 3-4 days. Within 5-10 days, the virus spreads to pharyngeal fluid and tissues. Since the virus persists in the pharyngeal region, half of the animals, even those that were vaccinated, become long term carriers (Golde, 2005).

1.4.3 Vaccines for FMD

Early studies of FMD vaccine development was initiated in late 1800s. FMD was the first described animal virus and the vaccine was the first animal vaccine to be developed (Lombard, 2007). However, the presence of various serotypes and unpredictable risk of viral virulence were the main problems of FMD vaccines. In 1937, Waldmann *et al*. were the first to inactivate the virus collected from vesicular fluids of infected cattles with formaldehyde to be used as a vaccine.

However, inactivation with formaldehyde causes incomplete viral inactivation and this problem was solved by the introduction of BEI (binary ethyleneimine)

inactivated antigens. The current vaccines against FMD are produced by infecting BHK-21 cells with live velogenic FMDV under bio-secure conditions and inactivation by using a chemical such as binary ethyleneimine (Rodriguez, 2009). Despite these improvements, the inactivated vaccines have a short shelf life and there is a need for vaccine cold chain. Moreover, there are difficulties with certain serotypes and subtypes to grow well in cell culture for vaccine production (Hu, 2007).

Additionally, the basic technology for vaccine production is unsafe, requiring the growth of large volumes of virulent FMDV, subsequent virus inactivation, antigen concentration and purification. At this stage the method of concentration of the antigen is a concern. Aluminum hydroxide gel adsorption, or polyethylene glycol precipitation methods are still used in some parts of the world, failing to eliminate unwanted cellular protein contaminants and viral non-structural proteins which may cause allergic responses in vaccinated animals (Doel, 2003).

There are “hot spots” where viral activity persists over long periods of time in the local population (Table 1.5). Generally, these spots are located in poor countries that do not have sufficient veterinary services and income needed for control and elimination of the disease (Sumption, 2008). Thus, the cost of vaccination is an important issue. On the other hand, current FMD vaccines do not induce broadly reactive long-term protection. Multiple vaccinations are required to maintain good levels of sustained immunity and periodic inclusion of new viral strains into the vaccine formulation is needed to cover new viral subtypes against which existing vaccines no longer protect.

There are ongoing trials and applications of novel vaccines developed against FMD based on more advanced methods such as recombinant protein and peptide vaccines, empty capsid vaccines and DNA vaccines. However, a number of results indicate

that there are limitations as well as benefits of these novel vaccines. Table 1.6 summarizes the advantages and disadvantages of different FMD vaccine types (Zhang, 2011).

Table 1.6 Advantages and disadvantages of different novel FMD vaccines (Adapted from Zhang, 2011)

Novel vaccines	security of production	security of vaccinated animal	shelf life	duration of immune response	vaccination effectiveness	Differentiation of infected animals from vaccinated ones
Subunit vaccine	Yes	Yes	Normal	Normal	Low	Yes
Live vector vaccine	Yes	Yes	Normal	Long	High	Yes
Nucleic acid vaccine	Yes	Risk to recombinant to other genomes	Long	Long	Low	Yes
Novel attenuated vaccine	Yes	Risk to toxicity reversion but low	Normal	Long	High	Yes
Synthetic peptide vaccine	Yes	Yes	Normal	Short	Low	Yes

The commercially available inactivated FMD virus vaccine produced in our country fails to provide long-lasting immunity, necessitating development of better vaccines that can specifically induce immunological memory. In this study, we aimed to delineate the immune adjuvant properties of CpG ODN/cationic peptide complexes to boost the immunogenicity of the FMD vaccine that can provide longer lasting immunity and better protection against the disease.

1.5. Aim of the study

Numerous pre-clinical studies show that CpG ODN are effective as vaccine adjuvants and that they synergistically enhance tumor regression when used in combination with surgery, chemotherapy and/or radiotherapy. Based on such findings, several dozen clinical trials utilizing CpG ODN have been conducted.

Unfortunately, clinical results suggest that CpG ODN are somewhat less potent in humans than in rodents (Nierkens, PloSone, 2009; Schmidt Biotechnol, 2007).

However, almost all human clinical trials employed included K-ODN. Since this ODN group cannot stimulate IFN-α secretion, a master cytokine that activates CD8-positive cytotoxic T lymphocyte responses (Schwartz, 2003) in humans, there is an urgent need to develop D-ODN mimetics that can be tested in clinical trials as anti-viral, anti-cancer agents and immune stimulatory vaccine adjuvants. Here, based on a simple complexation strategy with cationic peptides, we aimed to develop a K-ODN-based formulation that triggers high levels of IFNα in human blood. The study involves characterization of complexes, their immune stimulatory activity in human and mice and demonstrates their applicability as novel vaccine adjuvants.

CHAPTER 2

MATERIALS AND METHODS

2.1 Materials

2.1.1. Reagents

Cytokine ELISA kits including monoclonal unlabeled and biotinylated antibodies, recombinant cytokines, streptavidine-alkaline phosphatase (SA-AP)s were purchased from BioLegend (USA) and Mabtech (USA). Substrate for alkaline phospahatase, *p*-nitrophenyl phosphate disodium salt (PNPP) was purchased from Thermo Scientific, (USA). Immunoglobulin ELISA reagents; goat anti-mouse IgG, IgG1, IgG2a monoclonal antibodies conjugated with alkaline phosphatase (AP) were obtained from Southern Biotech (USA). Fluorescence labeled antibodies were from purchased BioLegend (USA). 100-1000 bp DNA ladder was from BioLabs (USA).

2.1.2. TLR Ligands, ODNs and Peptides

TLR ligands for stimulation assays were as follows and supplied from several vendors: peptidoglycan (PGN) isolated from *B.subtilis*; (Fluka, Switzerland), lipopolysaccharide (LPS) (isolated from *E.coli*; Sigma, USA), poly inosinic acid: cytidylic acid (pIC) (Amersham, UK) CpG and control GpC ODNs were synthesized by Alpha DNA (Montreal, Canada), and was kind gift by Dr. Dennis M. Klinman (NCI/NIH, USA). All ODNs were free of endotoxin and protein. Short cationic peptides were synthesized by Anaspec (USA). Sequences of CpG ODNs and cationic peptides used are summarized in Table 2.1.

Table 2.1 CpG ODNs and cationic peptides that were used in complexation and stimulation experiments. Bases shown in capital letter have phosphorothioate and those in lower case have phosphodiester backbone. CpG or flip (GpC) motifs are underlined.

CpG ODN		**Sequences**
K23 (12 mer)		TCGAGCGTTCTC
D35 (20 mer)		GGtgcatcgatgcaggggGG
K23 flip (12 mer)		TCGAGGCTTCTC
Peptides	**Charge**	**Sequences**
KR12 (12 mer)	+4	KRIVQRIKDFLR
LL37 (37 mer)	+6	LLGDFFRKSKEKIGKEFKRIVQRIKDFLRNLVPRTES
TAT (11 mer)	+8	YGRKKRRQRRR

2.1.3. Cell Culture Media, Buffers and Other Standard Solutions

DNAse/RNAse free water, RPMI1640 and low glucose DMEM media, Na-pyruvate, HEPES, L-glutamine, penicillin/streptomycin, non-essential amino acid solution, FBS were from Hyclone (USA). Components of various culture media and different buffers are given in detail in Appendix A.

2.2. Methods

2.2.1. Preparation of Complexes

2.2.1.1. Self-assembly of CpG ODN/Peptide Complexes

CpG ODN K23 (12-mer), K3 (20-mer) or their GpC (flip) controls were mixed at different molar ratios (1:1, 1:2, 1:4, 1:8, 1:16) with the anti-microbial cationic peptide LL37 (37-mer; +6 charge), its shortest active derivative KR12 (12-mer; +4 charge), or Tat peptide (11-mer; +8 charge) as shown in Appendix B. Complexes were incubated for 30 min at RT and were used for stimulation experiments following dilution in cell culture medium.

2.2.2. Characterization of Complexes

2.2.2.1 Demonstration of Complexation Using Agarose Gel Electrophoresis

To confirm that CpG ODN formed complexes with the cationic peptides, 20 μl of each complex (concentration based on ODN amount) was mixed with 4 μl of 6X loading dye (Appendix A) and the resultant mixture was loaded into wells of a 1% agarose gel containing 1mg/ml ethidium bromide. Uncomplexed CpG ODN (1.6 μg) was also applied as the negative control. DNA ladder with 100-1000 bp range (Fermantas) was used as a marker (3 μg/well). Electrophoresis was carried out using 1X TAE buffer (Appendix A) at 70 V for 60 minutes. The gels were visualized under a UV transilluminator (Vilber Lourmat, France). The gel exposure time was kept fixed at 70 sec for each run. Each experiment was repeated for a minimum of 3 times using a new batch of complexes.

2.2.2.2. Average Particle Size Analysis and Zeta Potential Measurements

CpG ODN/Peptide complexes were prepared as described above and kept at +4°C . 24 hours later complexes were diluted 50X with DNase/RNase free H_2O and 1ml of this solution was placed into a polystyrene cuvvette. For Zeta potential measurement,

a disposable capillary cell was used. Zeta potential, average particle size and polydispersity indexes were measured on a Zetasizer (Nano ZS, Malvern, UK) using dynamic light scattering technique. All measurements were carried out using the following parameters: medium refractive index 1.330, medium viscosity 0.88 mPa s, dielectric constant 78.54, temperature 25℃. The same procedure was repeated for size measurement using fresh complexes (within 2 h of preparation) to compare changes in stability over time. Measurements were in duplicate, and the results were expressed as the average of two measurements ± standard deviations.

2.2.2.3 Atomic Force Microscopy (AFM)

To obtain information about the substructure and topography of complexes, AFM studies were performed. The most stable molar ratios of CpG ODN/Peptide complexes (as determined by dynamic light scattering and zeta potential measurements) were prepared as before and diluted 1000X in DNase/RNase free H_2O. Complexes were deposited on to silicon wafers (5µl) and were allowed to dry at room temperature for 30 min. Images were taken at non-contact mode using a XE-100E model AFM (PSIA with XEI 1.6 software incorporated). Multi75Al model tips were from Budget Sensors. Tips' resonance frequency and force constant were 75 kHz and 3 N/m, respectively. Scan rate was kept at 0.73-0.79 Hz. The scanned area sizes were in 1 X 1 mm range. Images were analyzed using XEI 1.6 software.

2.2.3 Cell Culture

2.2.3.1. Cell Lines

2.2.3.1.1. RAW 264.7

RAW 264.7, murine macrophage like cells were cultured in complete RPMI 1640 containing 10% FBS and cells were passaged every 3-4 days upon reaching >80% confluency.

2.2.3.1.2. CAL-1

CAL-1 cells, a human plasmacytoid dendritic cell (pDC) like cell line, were cultured in complete RPMI 1640 plus 10% regular FBS and were passaged every 2 days by diluting 1:10 in fresh media.

2.2.3.2 Preparation of Human Peripheral Blood Mononuclear Cell (hPBMC) from whole Blood

Blood samples from healthy donors were collected into anti-coagulant containing (Sodium Citrate, EDTA or Heparin) tubes. 15 ml of Histopaque density separation solution (Biochrom AG, Germany and Sigma USA) was placed into a 50 ml falcon tube and 22.5 ml anti-coagulant treated blood was slowly layered on top of Histopaque without disturbing layers. Samples were centrifuged at 1800 rpm for 30 minutes with the break off at RT. The cloudy buffy coat at the interphase, peripheral mononuclear cells and basophiles were collected using a sterile Pasteur pipette and transferred to a new tube. Samples were washed twice in 50 ml 2% FBS supplemented regular RPMI medium followed by centrifugation at 1800 rpm for 10 minutes. The resultant cell pellet was resuspended in 10 ml of complete medium and the cells were counted as described in Section 2.2.3.4.

2.2.3.3 Preparation of Single Cell Suspensions from Spleen

2.2.3.3.1 Maintenance of Animals

Adult male or female BALB/c (8-12 weeks old) mice were used for all *in vitro* stimulation and *in vivo* immunization experiments. The animals were kept in the animal holding facility of the Department of Molecular Biology and Genetics at Bilkent University under controlled ambient conditions (22 ^{o}C ±2) regulated with 12 hour light and 12 hour dark cycles. They were provided with unlimited access of

food and water. Our experimental procedures have been approved by the animal ethical committee of Bilkent University (Bil-AEC).

2.2.3.3.2 Preparation of Single Cell Suspensions from Spleen

Female BALB/c mice were sacrificed via cervical dislocation and spleens were removed and placed into a 35cm petri dish containing 3ml of complete RPMI supplemented with 2% FBS. Single cell suspensions were obtained by smashing the spleens with the back of a sterile syringe plunger using circular movements under sterile cell culture conditions. Homogenous part of media was collected using a sterile plastic pasteur pipette while cell clumps belonging to fibrous or connective tissue were left in the petri dish. The cells were washed 2-3 times in complete RPMI followed by centrifugation at 1700 rpm for 10 minutes. After the final washing step, cells were counted and resuspended in complete RPMI supplemented with 5% FBS.

2.2.3.4 Cell Counting

At the end of the washing steps, cells were spun down, supernatants were aspirated and pellets were resuspended in 10 ml of complete RPMI 1640 media. Cells were diluted 10 fold and applied onto a hemocytometer. Cells in 4 corners (composed of 16 small squares) with 1 mm^2 area were counted under a light microscope and the cell number was calculated by the formula:

$$\frac{\text{Total cell number in 4 big squares} \times 10 \times 10^4}{4} = \text{number of cells per ml}$$

Working cell concentration was adjusted to 4×10^6 cells/ml for ELISA, 1×10^7 cells/ml for RNA extraction and 2×10^6 cells/ml for FACS analysis, unless otherwise stated.

2.2.4. Determination of Immunostimulatory Activity of Complexes

2.2.4.1. In vitro Stimulation of Cells with CpG ODN/peptide Complexes

CpG/ODN-peptide complexes were prepared at least 30 min before the experiment as described in Section 2.2.1.1. For stimulation in 96-well cell culture plates, 100 µl from a $4x10^6$ cells/ml stock (400,000 cells/well) were transferred to each well. Final volume in each well was adjusted to be 200 µl following addition of ODNs or complexes in 100 µl 10% FBS supplemented complete medium. Stimulations were performed in duplicate wells for each treatment. For stimulation in 15 ml falcon tubes, 100 ul of $10x10^6$ cells/ml stock (1,000,000 cells/tube) plus 100ul of stimulant were completed to 1ml final volume with 10% FBS supplemented complete medium. Depending on the identity of the cytokine intended for measurement, cell culture supernatants were collected following 24-48h of incubation. For gene expression studies, incubation periods were kept at 1-6 hours while for FACS analysis, cells were stimulated for a period of 6-72 hours depending on the marker/cytokine to be examined.

2.2.4.2 Enzyme Linked-ImmunoSorbent Assay (ELISA)

At the end of each incubation period, 96 well tissue culture plates were spun at 1700 rpm for 5 min and ~180 ul of supernatants were collected and stored at -20°C until use. 96-well PolySorp plates (F96 Nunc-Immunoplate, NUNC, Germany) or Immulon 2B plates (Thermo Labsystems, USA) were coated with monoclonal antibodies against mouse or human cytokines. Working concentrations of coating antibodies for each cytokine used are given in to Table 2.2. Each antibody solution was added at a volume of 50 µl/well and the plates were gently tapped for uniform spreading. Plates were incubated at room temperature for 4 hours or at 4°C overnight, followed by blocking in 200 µl blocking buffer (Appendix A) for 2 h at room temperature. Plates were washed with ELISA wash buffer 5 times with 5 minute incubation intervals and then rinsed with ddH_2O for 5 times and dried by

tapping. 50 µl of supernatants and recombinant cytokine standards were added into the wells. Starting concentrations for human and mouse recombinant cytokines are given in Table 2.2. Recombinant cytokines were serially diluted two-fold with 50 µl 1X PBS (11 such dilutions were made). Plates were incubated for 2-3 hours at room temperature or overnight at 4°C and were washed as previously explained. 50 µl of 1:1000 diluted (in T cell buffer; see Appendix A) biotinylated-secondary antibody solution was added into wells and plates were incubated 2-3 hours at room temperature or overnight at 4°C. Plates were washed as before and 50 µl of 1:5000 diluted streptavidin-alkaline phospahatase solution (SA-AP) was added to each well. The streptavidin-alkaline phospahatase solution must be prepared at least 2 h prior to its use to ensure uniform color development. Plates with SA-AP were incubated for 1 hour at room temperature followed by washing as before. To develop the plates, a PNPP tablet was dissolved in 4 ml ddH_2O and 1 ml PNPP buffer and 50 µl of this solution was transferred to each well. Color development was followed at 405 nm over time using an ELISA reader, Multiskan FC Microplate Photometer (Thermo Scientific, USA) until recombinant cytokine standards reached a four parameter saturation and yielded an S-shaped curve. Cytokine concentration of each sample was calculated using the corresponding standard curves.

Table 2.2 Antibodies and recombinants used in ELISA

Coating Antibodies	**Working Concentration**	**Recombinants**	**Starting Concentration**
Ab-hIFNα (MabTech, Sweden)	5 µg/ml	rec-hIFNα (MabTech,Sweden)	250 ng/ml
Ab-hIP10 (BD Biocience, USA)	2 µg/ml	rec-hIP10 (BD Biocience, USA)	-
Ab-mIFNδ (MabTech, Sweden)	1 µg/ml	rec-mIFNδ (MabTech, Sweden)	100 ng/ml

2.2.4.3 Fluorescence Activated Cell Sorting (FACS)

2.2.4.3.1 Fixation of Cells

Following the end of each incubation period, cells were centrifuged, aspirated and the pellets were fixed with the addition of 100 µl of 4% paraformaldehyde (Invitrogen, USA) while vortexing. Following incubation for 15 min at RT, cells were washed using 1 ml PBS-BSA-Azide (FACS Buffer; Appendix A) and cell suspensions were transferred into 1.5 ml tubes. Supernatants were discarded following centrifugation and aspiration as described above and the pellets were resuspended in FACS Buffer containing labeled antibodies as described in the following section.

2.2.4.3.2 Cell Surface Marker Staining

Fixed or live cells were centrifuged and supernatants were discarded. Pellets were resuspended in 100 µl FACS buffer containing 1ug/ml of fluorochrome conjugated antibody (against various cell surface markers) and were incubated in dark for 30 min. Fixed cells were incubated at RT whereas for live cells all incubations and washing steps were conducted at 4°C. Antibodies against the following cell surface markers were used throughout this thesis as summarized in Table 2.3. Following staining, cells were washed twice with FACS Buffer, resuspended in 400ul of PBS and analyzed on a BD^{TM} Accuri C6 Flow Cytometer.

Table 2.3 Fluorochrome conjugated antibodies used against cell surface markers

PE ab-h TNFα	(Biolegend, USA)
PE/Cy5 ab-h CD123	(Biolegend, USA)
FITC ab-h BDCA2	(Biolegend, USA)
PE ab hCD83	(Biolegend, USA)
PE/Cy5 ab h CD86	

2.2.4.3.3 Intracellular Cytokine Staining

For intracellular TNFα staining, all stimulations were done as before except the addition of 10ug/ml Brefeldin A (Biolegend) to prevent cytokine secretion into the medium. Following incubation for 5 hours at 37°C, cells were pelleted by centrifugation and were fixed and washed as previously described. The cells were permeabilized and stained simultaneously using 100 µl permeabilization medium (Invitrogen, USA) containing 0.5 µg of biotinylated antibody against TNFα (Pierce, USA) in dark for 30 minutes. Then, after washing, cells were incubated with 1:500 diluted SA-PE conjugate (BD Pharmingen) in 100 µl permeabilization medium in dark for 30 minutes and washed twice more prior to analysis on a BD^{TM} Accuri C6 Flow Cytometer.

2.2.5. Determination of Gene Expression at mRNA Level

2.2.5.1. Total RNA Isolation

All experimental steps were carried out on ice and all centrifugations were at 4°C. The minimum initial cell number was $5x10^6$ for each treatment. Following indicated times of stimulation, cells were centrifuged at 1700 rpm for 10 minutes, supernatants were discarded and pellets were treated with 1 ml Trizol, a mono-phasic solution of phenol and guanidinium thiocyanate (Invitrogen). For 1 mL of Trizol, 200 µl of chloroform was added to each tube and the tubes were shaken vigorously for 15 seconds. After they were incubated at room temperature for 3 minutes, samples were centrifuged at 13200 rpm for 15 minutes at 4°C. 650 µl of the clear upper aqueous phase containing total RNA was transferred to a new tube and 500 µl isopropanol was added, followed by gentle shaking. Tubes were incubated at room temperature for 10 minutes and centrifuged at 13200 rpm for 15 minutes. The supernatants were discarded and pellets were gently washed with 1 ml of 75% ethanol. Samples were centrifuged at 8000 rpm for 7 minutes. Supernatant were discarded and pellet was

gently washed with 1ml >99.9% ethanol again. After centrifugation at 8000 rpm for 7 minutes, ethanol was discarded and pellet was dried under laminar flow hood in a tilted position. Dry pellets were dissolved in 20 µl RNase/DNase free ddH_2O. The OD measurements at 260 and 280 nm wavelengths were obtained using NanoDrop ND-1000 (NanoDrop Technologies, USA). DNA, protein, polysaccharides or phenol contamination was checked using A260/A280. RNA samples were then stored at -80°C until further use.

2.2.5.2. cDNA Synthesis

cDNAs were synthesized from total RNA samples with the cDNA synthesis kit (BioLabs) according to the manufacturers' protocol. 1 µg total RNA was mixed with 1 µl of Oligo(dT)15 primer (100 ng) and total volume was completed to 8 µl with RNase DNase free H_2O. Samples were pre-denatured at 65°C for 5 minutes in an MJ Mini thermocycler (BIO-RAD, USA) and then spun down. 10 µl RT Buffer (including dNTP mix and 10 mM $MgCl_2$) and 2 µl M-MuLV RNase H^+ reverse transcriptase (includes RNase inhibitor) were added to the mixture. Tubes were incubated at 25°C for 10 minutes, at 40°C for 45 minutes and at 85°C for 5 minutes. cDNA samples were stored at -20°C for further use.

2.2.5.3. Polymerase Chain Reaction (PCR)

Primers were designed using a Primer3 Input v.0.4.0 program (http://frodo.wi.mit.edu/primer3/input.htm) and Primer Designer Version 2.0 using the cDNA sequences of human and mouse genes available at the Ensembl database. Each primer pair was blasted (http://www.ncbi.nlm.nih.gov/BLAST/) against the mouse or human genome. Detailed information on mouse primers are given in Table 2.4.

Table 2.4. The Mouse Primers

Mx		Tm	GC%	product size
	F GTGCCCTATCAAGGGAATGA	60	50	485bp
	R TTGTAAGGGTGGAACCCAAG	60	50	

All reagents were mixed and subjected to optimal PCR conditions for specific primer sets in an MJ Mini thermocycler (Biorad, USA). PCR mixtures were prepared according to the protocol in Table 2.5. Running conditions for mouse primers are given in Table 2.6. PCR products were kept at 4°C until they were loaded onto 1% agarose gel.

Table 2.5 PCR mixture protocol

Reaction Ingredients	**Volume**
cDNA	1 µl
2X DyNAyzme™ II Master Mix (Finnzymes)	12.5 µl
Forward Primer (from 10 pmol stock)	1 µl
Forward Primer (from 10 pmol stock)	1 µl
Nuclease-free ddH2O (Hyclone)	9.5 µl
Total volume	25 µl

Table 2.6 PCR running conditions for mMx

95 °C	10 min	
1) 95 °C	30 sec	40x
2) 60 °C	30 sec	
3) 72 °C	30 sec	
72 °C	10 min	
4 °C	forever	

2.2.6. Determination of Cell-surface Binding and Internalization of complexes

CpG ODN/peptide complexes were prepared using FAM labeled K3 ODN as described in Section 2.2.1.1. CAL-1 cells (400,000 cells/well) were incubated with the complexes (0.16, 0.5 and 1.5 μM) in a 96 well cell culture plate. Cells were then washed and analyzed on a BD™ Accuri C6 Flow Cytometer. Following the initial acquisition for the detection of total FAM signal, cells were transferred to a new plate and an equal volume of trypan blue (1:10 diluted, HyClone) was added to all samples. Cells were analyzed on a BD™ Accuri C6 Flow Cytometer again to assess the amount of internalized ODN only. Trypan Blue addition eliminated the cell-surface bound FAM-signal and enabled us to quantitate only the internalized fraction.

2.2.7. Determination of Nuclease Resistance of Complexes Following DNAse Treatment

PBMC were isolated as described in Section 2.2.3.2 and cells were plated in 96-well plates (600,000 cells/well). Free CpG ODN and CpG ODN/peptide complexes were pre-treated with of DNAse I (from bovine pancreas, Roche) according to the manufacturer's specifications. Each reaction tube contained 11 U DNAse I, 10 μg K23 ODN, 20 μl enzyme buffer and 37 μl ddH_2O. Following incubation at room temperature for 10 minutes, the reaction was terminated in a thermo cycler at 75 °C

for 10 minutes. Cells were then stimulated with DNAse I treated and untreated complexes and CpG ODNs (1 μM) for 24 h. Cytokine production from culture supernatants were assessed by ELISA and the immunostimulatory activity of DNAse I treated and untreated groups were compared.

2.2.8. Cell Viability Assay

In order to study the potential cytotoxic effect of complexes, stimulated cells were stained with propidium iodide (PI), a cell impermeable dye that gains access into dead or dying cells only. RAW cells (a representative of murine cells) and CAL-1 cells (a representative of human cells) were plated at a concentration of 500,000 cells per well followed by stimulation with optimum concentrations of (1 μM) free CpG ODN, free peptides and their complexes for 24 hours at 37 °C. At the end of the incubation period, cells were pelleted and resuspended in 200 μl of 1X PBS containing 2 μl of PI (Millipore, USA). Cells were incubated for 15 minutes at room temperature in dark with this PI solution. Following washing with cold 1X PBS twice, cells were resuspended in 200 μl PBS and the cell-associated PI fluorescence was detected on a BD™ Accuri C6 Flow Cytometer. Percentages of PI positive cells (an indicator of dead cells) were compared between different groups.

2.2.9. Determination of Subcellular Distribution of CpG ODN/peptide Complexes by Confocal Microscopy

To evaluate the subcellular distribution of complexes, RAW cells (500,000cells/group) were incubated with Cy5 conjugated CpG ODN (1μM) and its complexes with LL37 (8 μM) or TAT (16 μM) peptides at 37 °C for 30 minutes in the presence of 75 nM of LysoTracker Red (Invitrogen, USA) (marker for lysosomal compartment), or 25 μg/ml Transferrin-texas red conjugate (Invitrogen, USA) (marker for early/recycling endosomes). All samples were washed twice and were

placed on slides prior to analysis on a laser scanning confocal microscope under a 63X objective (CARL Zeiss, LSM).

2.2.10. Immunization Studies

2.2.10.1. FMD Vaccine

FMD Vaccine was prepared and provided by the FMD Institute (Ankara, Turkey). This monovalent vaccine formulation contained FMDV O/TUR/07 inactivated antigen in double oil emulsion with montanide ISA 206 (Seppic, France).

2.2.10.2. Immunization Protocol with CpG ODN/peptide Complexes and FMDV Antigen

6-8 week old female BALB/c mice (5/group) were immunized 3 times (intraperitoneal (ip), day 0 and 15 and 180) using 5X lower dose of the optimal licensed monovalent vaccine (0.5 μg/mouse) alone or its combination with i) CpG ODN, ii) CpG ODN/anti-microbial cationic peptide LL-37 complexes or iii) CpG ODN/cationic peptide Tat complexes. CpG ODN dose/mice was adjusted so that each animal recieved a 5X lower dose (2 μg) of ODN than the optimal adjuvant dose used in mice (10 μg). Blood was collected from the tail vein 2 weeks after each immunization. Sera were prepared by centrifugation at 8000 rpm for 5 min and stored at −20 ˚C until use.

2.2.10.3. IgG ELISA

Antigen specific IgG1 and IgG2a antibodies produced in mice were detected by ELISA. Immulon 1B plates (Thermo Labsystems, USA) were coated with 50 μl of rabbit anti-Ser-O antibody (1:2000 diluted) in PBS-and incubated overnight at 4 ˚C. Blocking and washing steps were carried out as described in Section 2.2.4.2. Following washing, 1/20 diluted supernatant of the cell lysate of FMDV-infected

Baby Hamster Kidney (BHK) cells was added to the plates in PBS (50ul/well) and incubated overnight at 4 °C. 25-80X diluted mouse serum from each animal was added into wells of the first row and serially diluted 2-fold thereafter. After overnight incubation at 4 °C and washing, goat anti-mouse IgG1/AP or IgG2a/AP (Southern Biotech) were 1:3000 diluted in T-cell buffer and were added to plates (50ul/well). Following incubation and a final wash, PNPP substrate was added (Perbio Pierce, USA) and formation of yellow color was followed at OD 405 nm using an ELISA reader (Thermo Scientific, USA)

2.2.10.4 Detection of Antigen Specific IFNγ Production by ELISA

Six months after the first injection, mice were boosted for a third time in order to follow memory cell responses. One day after the booster injection, sera of the mouse were prepared as described the section 2.2.10.2. Serum IFNγ levels were detected by ELISA as described previously (Section 2.2.4.2). 2 µg/ml mouse anti-IFNγ antibody (Mabtech) was used for coating.

2.2.10.5 Determination of IgG Secreting Cell Frequency by Limiting Dilution Analysis

In order to determine the frequency of defined clones of B lymphocytes responding specifically to FMDV antigen, limiting dilution analysis (LDA) was performed. Six months after the first injection, mouse were boosted as described in Section 2.2.10.2. Immulon 1B plates (Thermo Labsystems, USA) were coated and washed as described for the IgG ELISA. Spleens from three animals (per group) were removed and single cell suspensions were prepared as described in Section 2.2.3.3. Cells were counted and the cell numbers were adjusted to be $20x10^6$ cells/ml. 220 µl from each cell suspension was added into the first row of the template plates (in duplicate) and 150 µl of complete RPMI medium was added to the remaining rows. 4X serial dilutions were then carried out. Previously coated plates were used as stimulation plates. 50 µl cells were transferred from the template plate to corresponding wells of

the stimulation plates. The final volume was completed to be 200 µl using 10 % FBS supplemented medium. Thus, starting from row1 and ending in row4, the cell concentrations in the stimulation plate were: $1x10^6$, $2.5x10^5$, $6.26x10^4$ and $1.56x10^4$. Microtiter plates were incubated on a level surface in a CO_2 incubator for 24 hours. Following the end of incubation, plates were washed with ddH_2O instead of PBS so that the attached cells would burst and be washed out. Detection antibodies, goat anti-mouse IgG1/AP and IgG2a/AP (Southern Biotech) were 1:3000 diluted in T-cell buffer and were added to wells. The substrate NBT/BCIP (Invitrogen, USA) was prepared as 4 ml NBT/BCIP and 1ml ddH_2O for one plate and 50µl substrate was added to the plates. Color change was followed using an ELISA reader. Dose response data was analyzed according to Poisson single-hit model. Breifly, of all wells from one group of mice, % of nonresponding wells were calculated and this value was plotted against the corresponding cell concentration. The best-fitted linear lines that intercepted the numeric value of 0.37 (corresponds to 37%), gave us the frequency of IgG1 or IgG2a producers.

3.2.11 Statistical Analysis

Statistical analysis for the treatment groups were conducted by IBM SPSS17 software. Student`s t-test was conducted between control (or naïve) versus treatment groups (two-tailed unpaired comparison). P values that were <0.05 were considered as statistically significant throughout these studies.

CHAPTER 3

RESULTS AND DISCUSSION

3.1 Self-assembly of CpG ODN/Peptide Complexes

Complexation of negatively charged CpG ODN and positively charged peptides was studied in experiments where K type CpG ODN were mixed with three different types of cationic peptides. Since the sequences of the peptides determine the net charge and hydrophobicity of each molecule and hence would affect the property of their complexes with CpG ODN, the helix-wheel models of the peptides and their physical characteristics were deduced using the software provided by the http://kael.net/helical.htm web site (Figure 3.1). The peptides (1 μM, 2 μM , 4 μM ,8μM and 16 μM) were mixed with a constant amount of K type CpG ODN (1 μM) and complexation was followed by agarose gel electrophoresis, dynamic light scattering and zeta potential measurements as described in the following sections.

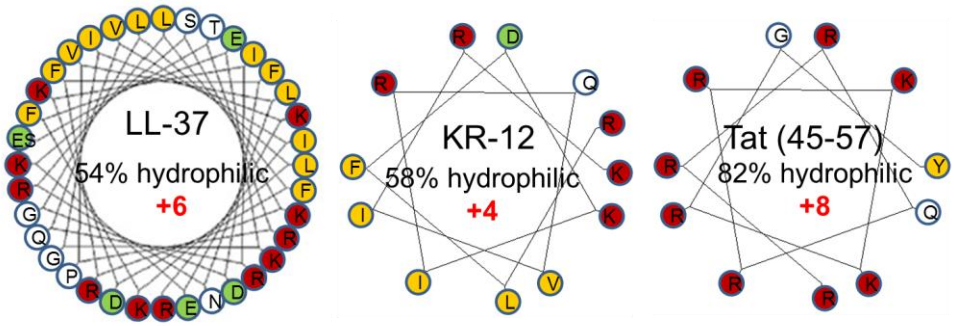

Figure 3.1 The helix-wheel models and physical characteristics of the cationic peptides used in this study. Yellow: Hydrophobic amino acids; Green: Negatively charged amino acids; Red: Positively charged amino acids.

3.1.1 Agarose Gel Electrophoresis

To determine whether complexation took place, various CpG ODN/peptide mixtures were loaded into the wells of an agarose gel and subjected to an electric field to force the negatively charged molecules towards the bottom of the gel. As expected, following complexation, the negatively charged phosphate groups of CpG ODN are gradually neutralized, the complexes remain in the wells and the signal from the free ODN is decreased. When band intensities of free ODN were compared to those obtained from complexes, (Figure 3.2), it was deduced that the CpG ODN/LL37 formed successful complexes when used at a molar ratio of 1:8. TAT peptide on the other hand, showed complexation even when used at a much lower molar ratio (1:4), possibly owing to its much higher positive charge density (+8). In the case of KR12, although band intensity seemed to be decreased with the increase of peptide amount, no complexes were seen in the wells. The mobility of the complexes in electrophoresis also depends on the size and shape of the molecule and it is conceivable that the movement of CpG ODN may be hindered as a result of aggregate formation. This simple agarose gel electrophoresis study of the complexes was undertaken to determine whether the molar ratios of CpG ODN:peptide would be sufficient to generate complexation. For a much clearer understanding of particle stability and size of the complexes formed, zeta potential measurements and dynamic light scattering analysis were performed.

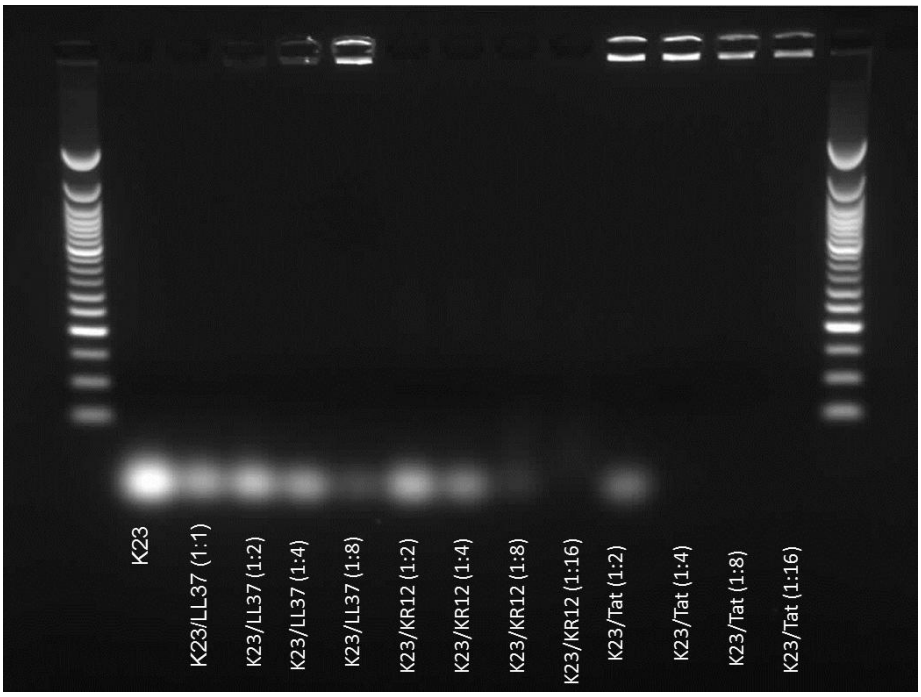

Figure 3.2 Agarose gel electrophoresis of CpG ODN/peptide complexes. CpG ODN (K23) and its complexes (1.6 μg each based on ODN amount) were loaded into wells of a 1% agarose gel containing. Uncomplexed CpG ODN demonstrates a bright signal whereas the signal disappears following successful complexation. DNA ladder with 100-1000 bp range was used as a marker (3μg/well). The gel image is a representative 3 independent experiments, each giving similar results.

3.1.2 Zeta Potential and Size Analysis of Complexes

Zeta potential is a physical property exhibited by particles in suspension and is an important indicator of stability of the particles in colloidal systems. It shows the amount of repulsion between similarly charged molecules. Therefore, if the zeta potential is very low, attractive forces surpass repulsive forces and particles will come together to form aggregates. Particles with large negative or positive zeta potentials that are small in size resist attraction and are hence electrically stabilized. In general, particles with zeta potentials larger than +30 or smaller than -30 mV are

considered as stable. Stability is also designated by the polydispersity index (PdI). In cases where PdI value is greater than 0.5, sample is too polydisperse, indicating the presence of very large or aggregated particles, reducing the suitability for dynamic light scattering measurements. In the light of the above information, zeta potential and dynamic light scattering analysis of the complexes were performed.

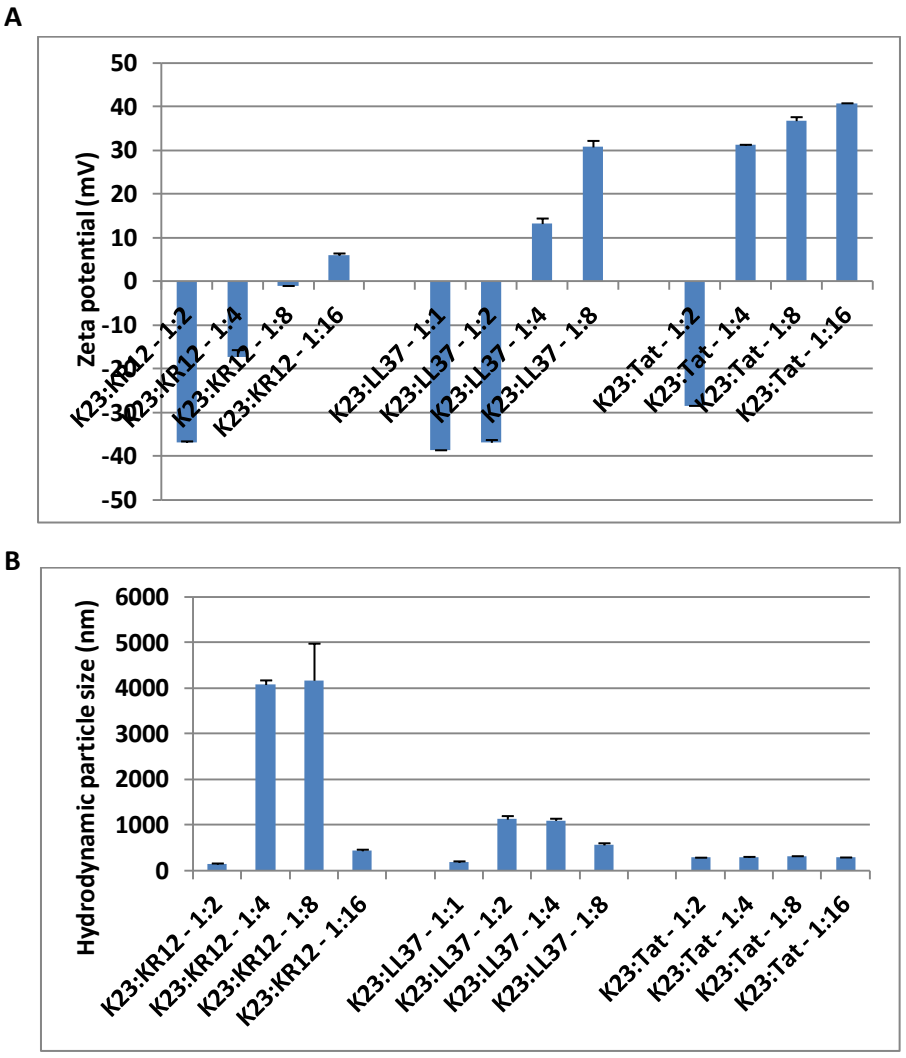

Figure 3.3 Zeta potential **(A)**, size **(B)** and polydispersity index **(C)** of complexes. Size change over time is given in **(D)**.

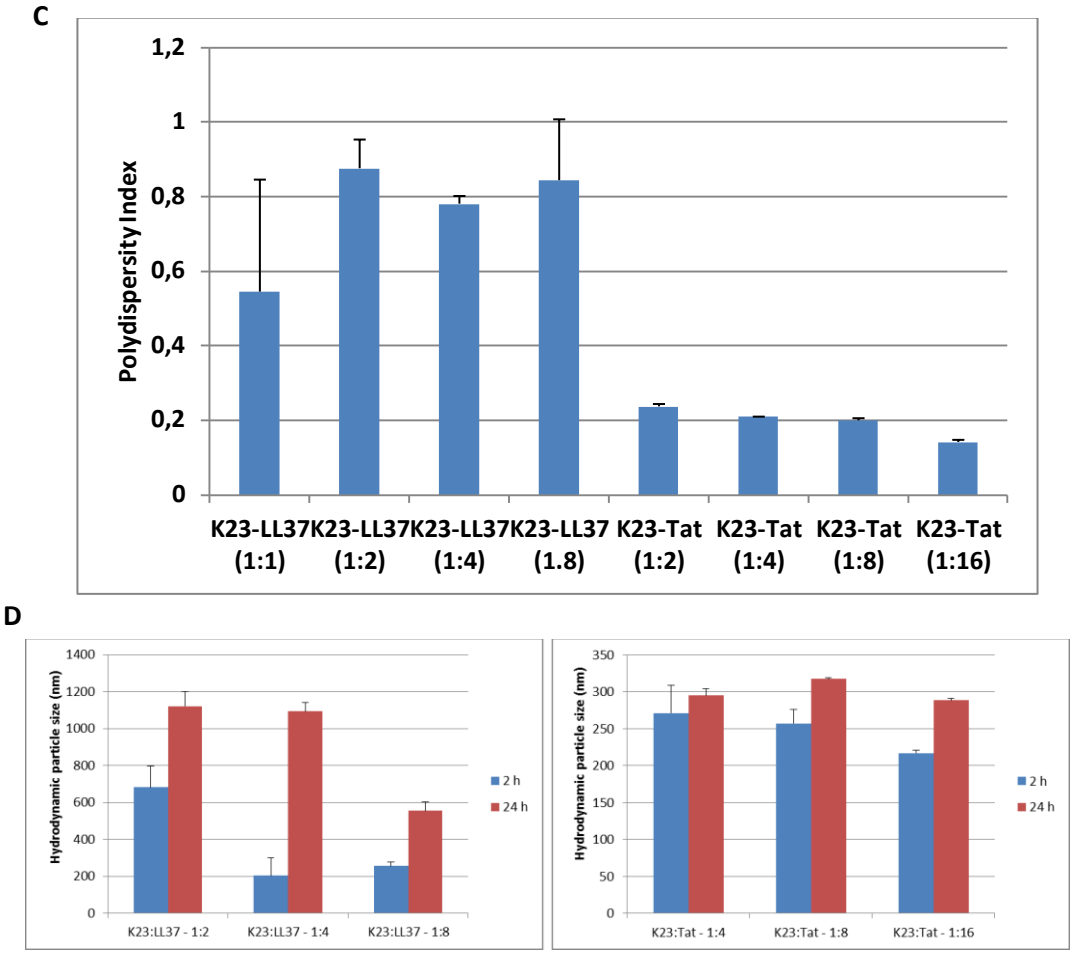

Figure 3.3 (cont'd) CpG ODN/peptide complexes were diluted 50X with DNase/RNase free H_2O. Zeta potential, average particle size and polydispersity indexes were measured on a Zetasizer using the following parameters: medium refractive index 1.330, medium viscosity 0.88 mPa s, dielectric constant 78.54, temperature 25°C. The results are given as the average of two replicates ± S.D.

As summarized in Figure 3.3, for all tested KR12 molar ratios, there was no stable complex formation with CpG ODN (maximum + zeta potential was 5.94 ± 0.54; Figure 3.2 (A)). The recorded hydrodynamic sizes were too large (4074 ± 101 nm and 4167 ± 814 nm; Figure 3.2 (B)), suggesting aggregate formation. LL37 peptide formed positively charged stable particles when used at a molar ratio of 1:8 (30.8 ± 1.48 mV; Figure 3.2 (A)). Particle sizes also showed great variability at different

ratios (Figure 3.3 (B)). In contrast, TAT peptide formed stable complexes with K23. Zeta potentials were -28.4 ± 0.00 mV, 31.2 ± 0.14 mV, 36.8 ± 0.92 and 40.7 ± 0.14 mV, for molar ratios of 1:2, 1:4, 1:8 and 1:16, respectively, with the highest ratio generating extremely stable complexes. Moreover, particle size data showed all combinations to yield similarly sized particles (~300 ± 20 nm) with uniform distribution (PdI ~0.2; Figure 3.3 (C)). The size of the formed nanoparticles did not change significantly over time (Figure 3.3 (D)) when Tat peptide was used but larger aggregates formed with LL37 at the end of 24 h. The representative individual Histograms of average size distributions of particles and their quality reports of stability are provided in Figure 3.4.

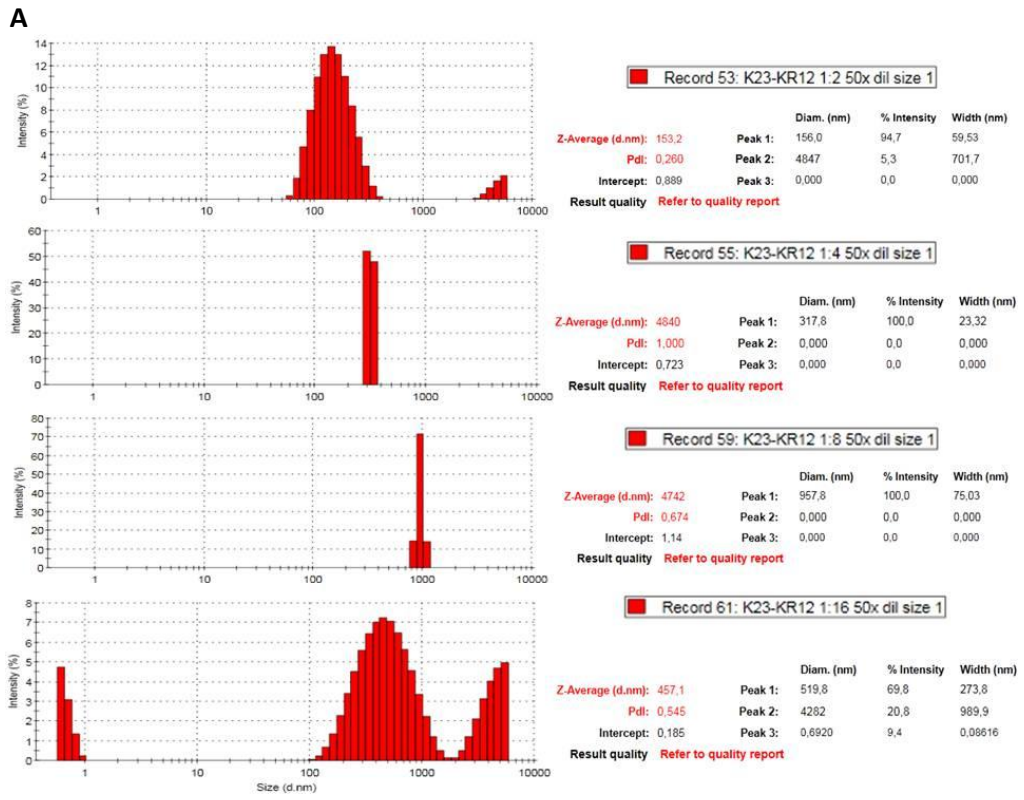

Figure 3.4 Histograms of average size distributions of particles with their quality reports of stability for complexes of CpG ODN and A: KR-12.

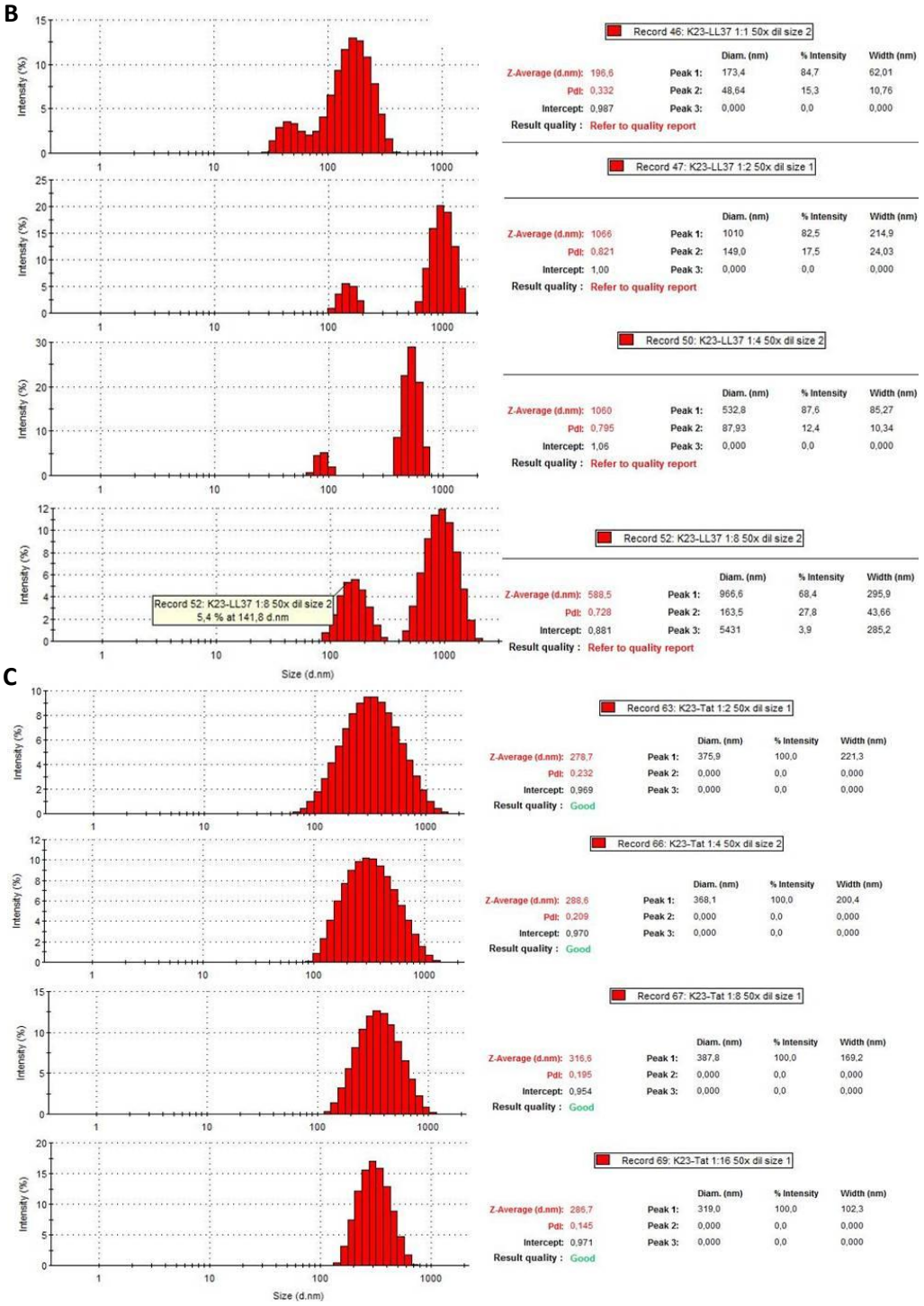

Figure 3.4 (cont'd) Histograms of average size distributions of particles with their quality reports of stability for complexes of CpG ODN and B:LL-37; C:Tat peptides.

3.1.3 Atomic Force Microscopy (AFM)

Morphology of the complexes was investigated with Atomic Force Microscopy (AFM). Different areas were scanned by the cantilever probe at non-contact mode and images were recorded for K23/TAT complexes (1:16). Detailed analyses of the AFM micrographs revealed that complexes demonstrated uniform-sized nanoparticles (Figures 3.5). While cantilever oscillations gave significant phase changes, the topography showed substantial altitude differences ranging from 10 to 20 nm. The morphology of the particles was not spherical but triangular. Previous results were supported by AFM analysis in terms of uniformity of the formed nanoparticles without aggregation and size of particles (~300 nm) were consistent with DLS data.

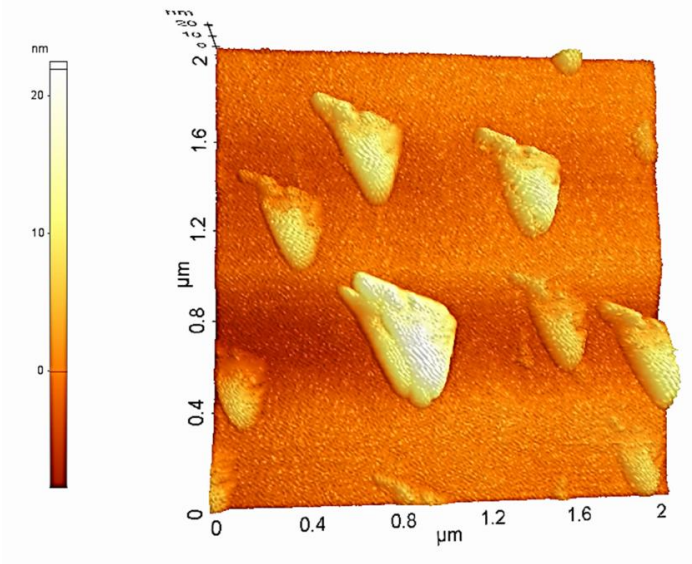

Figure 3.5 K23/TAT complexes (1:16) spontaneously form similar size nanoparticles. 5 µl aliquots from 1000X diluted complex solution were deposited onto silicon wafers. Non-contact mode AFM was set to investigate the topography. Scanned surface areas were 2 mm^2.

3.2 Immunostimulatory Activities of CpG ODN/peptide Complexes

As previously explained (Section 1.3.1), D Type ODNs trigger IFNα secretion from pDCs whereas K Type ODNs stimulate TNFα secretion from these cells (Gursel, 2002; Gursel 2006). The IFNα inducing activity of D Type ODN is closely related to its ability to form higher order structures. However, these complex multimeric structures complicate the GMP manufacturing process of this ODN class, preventing their entry into clinical trials. K Type ODNs were reported to induce type I IFN secretion from pDC following encapsulation in cationic liposomes or adsorption onto cationic nanoparticles (Bal, 2011; Yoshida, 2009) These approaches require expensive and tedious preparation steps that often include exposure to organic solvents and chemicals. Here, we wanted to explore the possibility of IFNα production by human pDCs following stimulation with K ODN/cationic peptide complexes. We further wanted to characterize the nature of the immune response elicited in human PBMC and mouse spleen cells.

3.2.1 Immunostimulatory Activities of CpG ODN/cationic peptide Complexes in hPBMC

The immune stimulation studies were carried out as described in Section 2.2.4.1. In order to determine the optimum activation conditions, preliminary experiments were conducted with complexes incorporating all 3 cationic peptides (KR12, LL37 and TAT), using four different K ODN:peptide molar ratios (1:2, 1:4, 1:8, 1:16; 1:1, 1:2, 1:4, 1:8 and 1:2, 1:4, 1:8, 1:16). The responses of 2 different PBMC preparations were tested using three different doses of CpG ODN (0,3μM, 1 μM and 3 μM). The IFNα levels present in culture supernatants were determined by ELISA following 24 hours of stimulation. Figure 3.6 summarizes the IFNα response of two different subjects stimulated with the complexes. As expected, the K type ODN (K23) failed to induce IFNα secretion at all doses (Figures 3.6 A, B and C). Similarly, its complexation with KR12 peptide was also unsuccessful (Figure 3.6.A). Therefore,

CpG ODN/KR12 complexes were eliminated from the rest of the studies. In contrast, K23/LL37 complexes induced significant IFNα production when used at 1 μM and 3 μM doses with the 1:4 and 1:8 molar ratios ($P<0.05$). Among the LL37 incorporating groups the best IFNα response was triggered by 1 μM K23/LL37 complex (1:4) (Figure 3.6.B). Similarly, 1μM and 3 μM doses of K23/TAT complexes at 1:8 and especially 1:16 ratios had considerable activity on hBPMCs in terms of IFNα stimulation ($P<0.05$) (Figure 6.3.C). The results also suggested that for both peptides, IFNα inducing activity correlated well with particle stability (coinciding with the highest CpG ODN/peptide ratios).

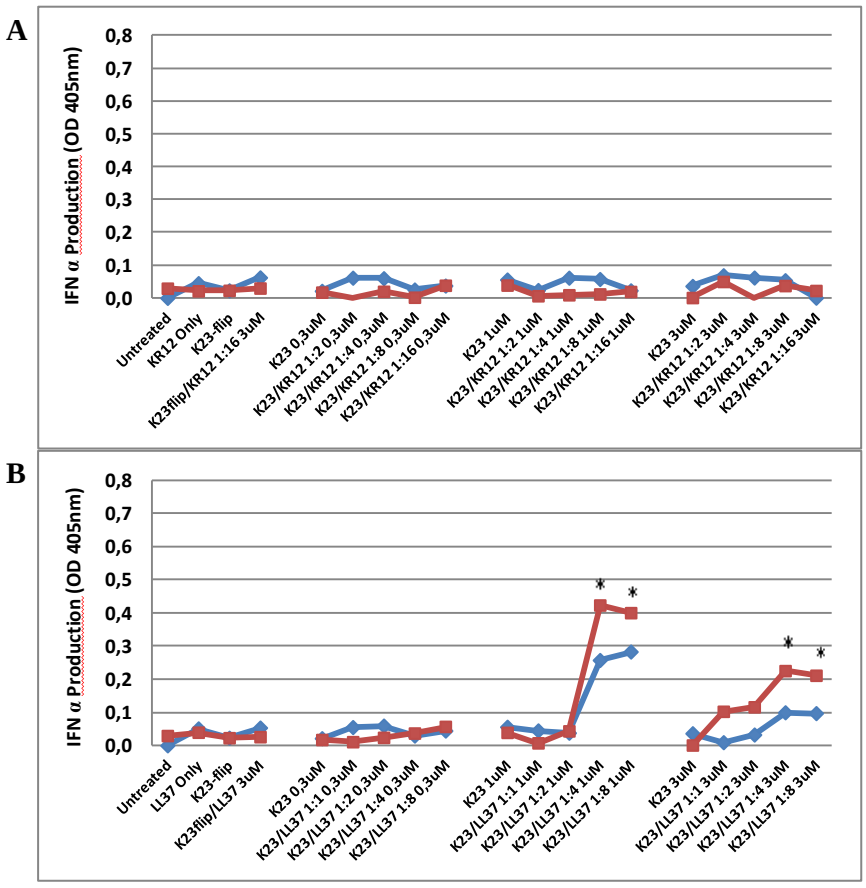

Figure 3.6 Dose dependent INFα production from hPBMCs (2 individuals) stimulated by K23/KR12 (A), K23/LL37 (B) and K23/TAT complexes (C).

C

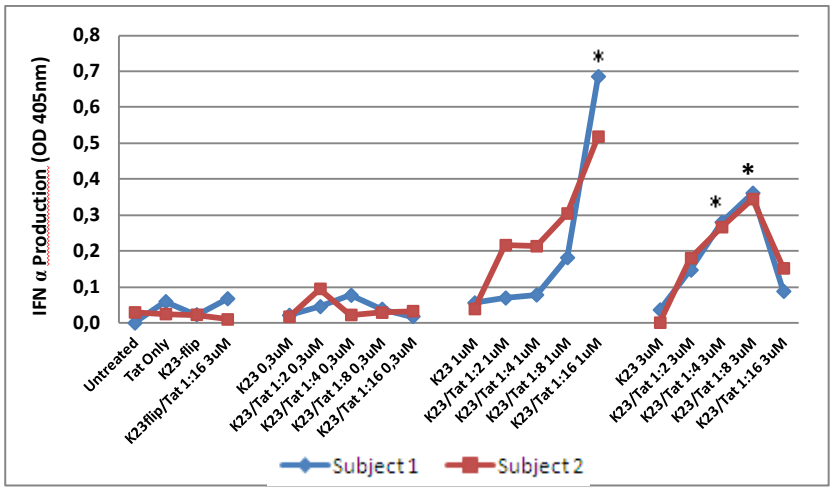

Figure 3.6 (cont'd) Cells were stimulated in duplicate and the average of the response induced by each formulation was compared to the same dose of K23 CpG ODN stimulated group. 1 μM and 3 μM of K23/LL (1:4; 1:8) (B) and K23/TAT (1:8; 1:16) (C) complexes produced significant amounts of IFNα with respect to 1 μM and 3 μM free K23. * indicates $P<0.05$.

Next, hPBMCs were isolated from 3-5 subjects and stimulated again with three different CpG concentrations and four different molar ratios of K23/LL37 and K23/TAT complexes. IP-10 and IFNα production was detected by ELISA 24 h later. IP-10 produced from 3 hPBMCs and IFNα results from 5 hPBMCs are illustrated in Figures 3.7 and 3.8, respectively.

Interferon gamma induced protein 10 (IP-10, also known as CXCL10), is a chemokine that attract macrophages, NK cells and T cells and critically contributes to anti-viral immunity. It plays an important role in clearance of viral infections (Lagging, 2006). Consistent with previous results, D type ODN (D35) and K23 induced moderate levels of this chemokine from the majority of the subjects (Figure 3.7 A and B). Complexation with cationic peptides, especially with Tat, boosted the levels of IP-10 produced significantly, even when the lowest dose of K23 was used

(0.3 μM). Highest level of IP-10 was induced by 1 μM ODN at the highest CpG ODN/peptide ratio (P<0.05) (Figure 3.7.A and B).

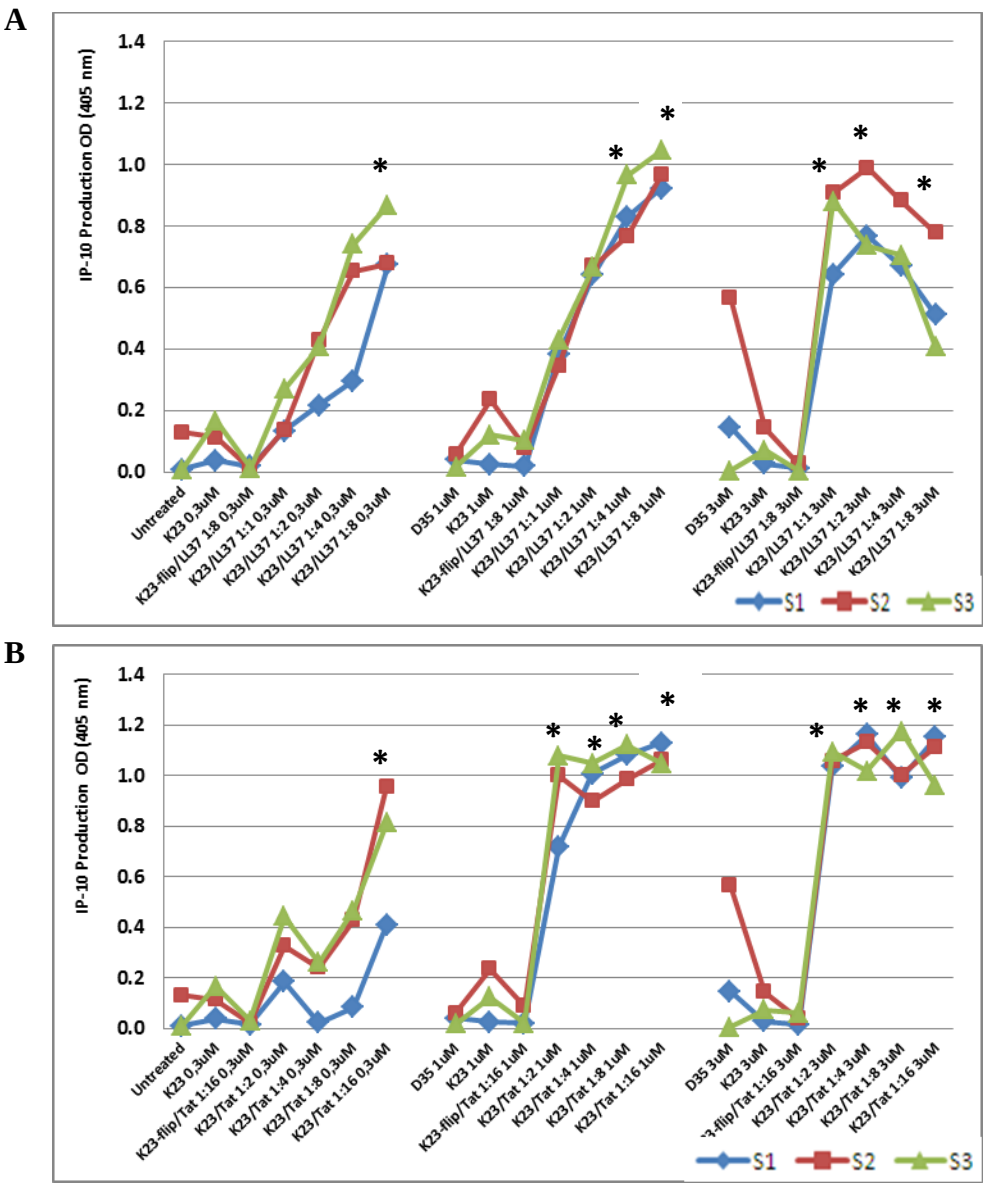

Figure 3.7 Dose dependent IP-10 production from hPBMC (3 individuals) stimulated by K23/LL37 (A) and K23/TAT complexes (B). Cells were stimulated in duplicate and the average of the response induced by each formulation was compared to the same dose of K23 CpG ODN stimulated group. * indicates P<0.05.

Human PBMCs produced the highest level of IFNα when they were stimulated with 1 μM of ODN in complexes. When the two complexes were compared at their highest molar ratios in terms of their IFNα stimulating capacity, K23/TAT was found to induce 2-5 fold more IFN than the LL37 incorporating complex ($P<0.05$, Figure 3.8).

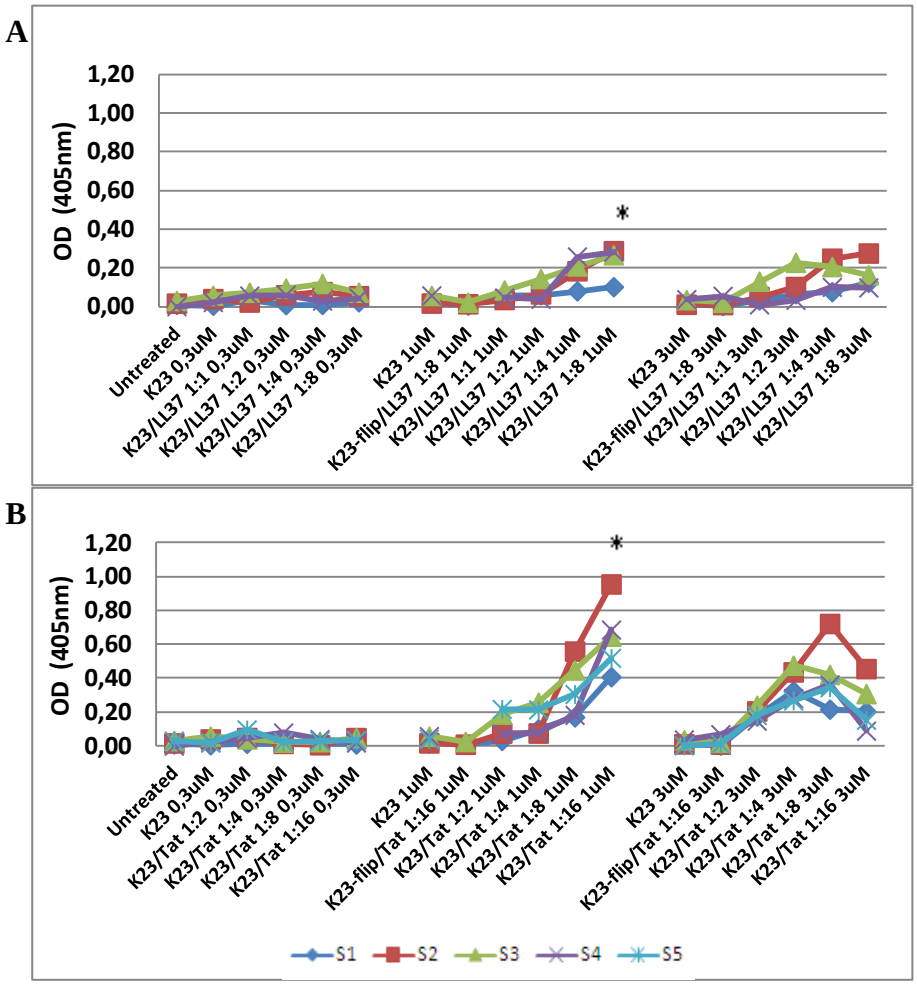

Figure 3.8 IFNα response of hPBMCs (5 individuals) stimulated with K23/LL37 (A) and K23/TAT complexes (B). Cells were stimulated in duplicate and the average of the response induced by the highest molar ratio of CpG ODN/peptide between LL37 and Tat containing groups were compared (1 μM). * indicates $P<0.05$.

Previous work showed that K type ODN but not D type induced tumor necrosis factor (TNFα) from human pDCs. To test whether K23 in the complexes still induced this cytokine or shifted to a complete D-type immune stimulatory profile, hPBMC were stimulated with K23 or its complexes for 5 hours in the presence of brefeldin A, a chemical that aids cytokine accumulation within the target cell to enable its detection by flow cytometry. Following stimulation, pDCs in human PBMC were stained with specific markers (CD123 and BDCA-2), permeabilized and stained for TNFα production using PE labeled anti-TNFα antibody. The results are shown in Figure 3.9.

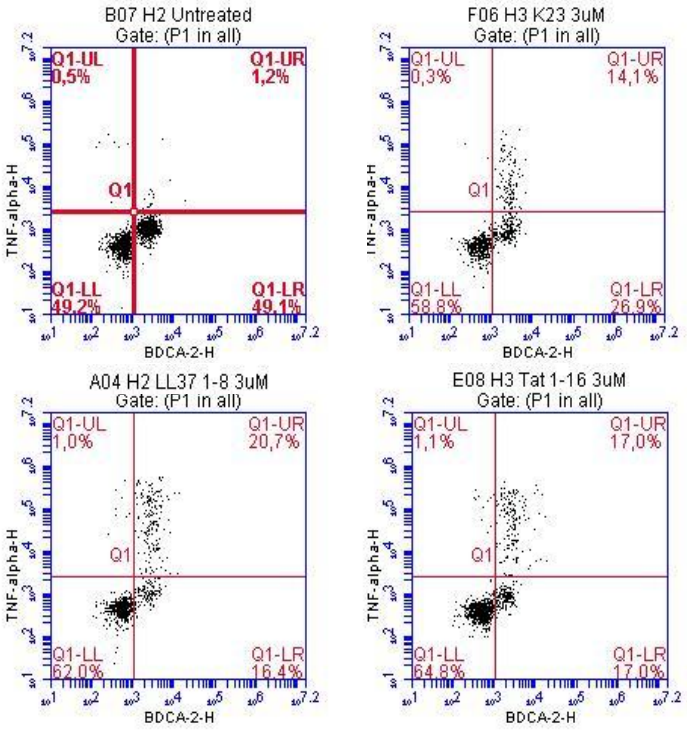

Figure 3.9 Intracellular cytokine staining of TNFα produced in pDCs stimulated without or with free K23 or its complexes. The results are the representative of 3 PBMCs stimulated with similar results.

As seen from the figure, both K23 and its complexes stimulated TNFα production from CD123 gated BDCA-2 positive cells (upper right quadrants). Unstimulated cells gave a background level of 1.2% TNFα production whereas with K23, LL37 complex and Tat complex, cytokine producers increased to 14.1, 20.7 and 17.0 %, respectively. These results suggest that in contrast to D type ODN that can stimulate IFNα but not TNFα from pDCs, and K type ODN that can stimulate TNFα in the absence of any IFNα, the complexes of K23 could trigger both cytokines simultaneously, combining the best aspects of both ODN class.

T and B cells need two signals to be activated. An antigen-specific first signal is supplied through the interaction of receptor and peptide-MHC complex on the antigen presenting cells (APCs). An antigen nonspecific second signal, the co-stimulatory signal is provided by the interaction between co-stimulatory molecules of APC and the effector cells (Jahrsdörfer, 2001). CD83 is a maturation marker for human dendritic cells (DCs). During DC maturation, CD83 is upregulated together with co-stimulatory molecules such as CD86 on these cells. Thus, we further tested the upregulation of these molecules in PBMC by flow cytometry 24 hours following stimulation (Figure 3.10). Briefly, whereas K23 induced only a 1.5 fold increase in the number of CD83/CD86 double positive cells in comparison to the unstimulated control, its complexes with LL37 and Tat induced a 4-fold and 5-fold increase in the percentages of these cells (upper right quadrants, Figure 3.10).

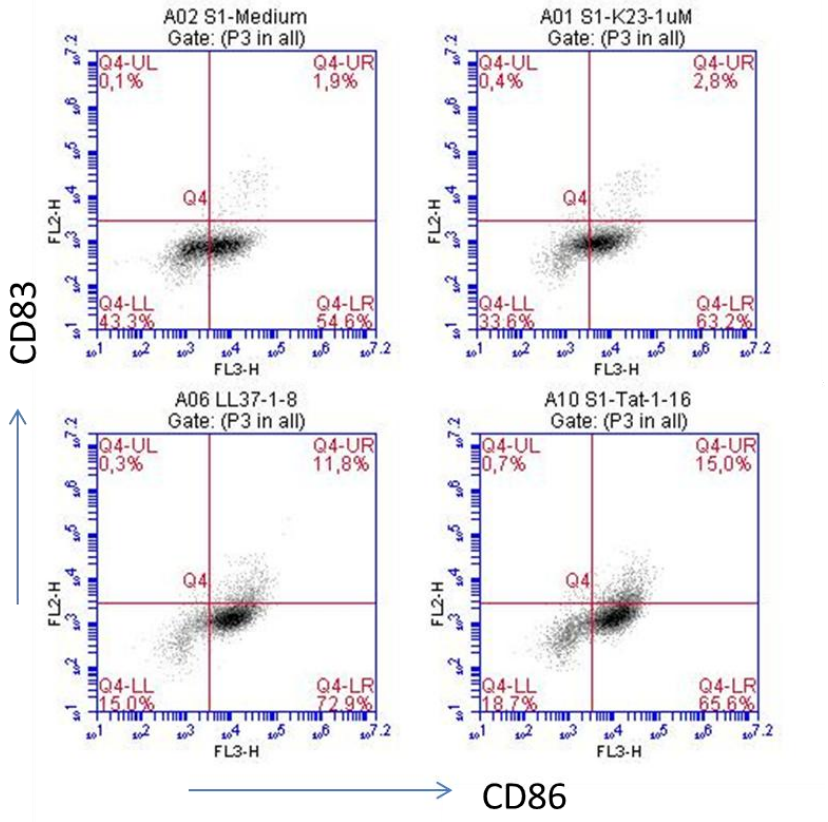

Figure 3.10 Increase in costimulatory molecule (CD86) and DC maturation marker (CD83) expression in response to stimulation with 1 μM K23 or ODN/peptide complex 24 hours following stimulation. Cells were stained with fluorescent dye conjugated markers and double positive cells were analyzed by flow cytometry. The results are the representative of 3 PBMCs stimulated with similar results.

3.2.2 Immunostimulatory Activities of CpG ODN/cationic peptide Complexes in Mouse Splenocytes

In order to verify that the complexes also showed immunostimulatory activity in mouse, we followed the expression of 2 important proteins: First, the Mx protein transcript was followed by semi-quantitative PCR as an indicator of anti-viral activity. Next, IFN gamma production was followed by ELISA.

The Mx proteins are induced specifically by Type-I IFNs. Mx proteins are usually located in the cytoplasm, and are known to have an antiviral effect via targeting specific steps of the viral replication cycle (Müller, 2002). Therefore, they are considered as Type-I IFN indicators. Single cell mouse Splenocytes were stimulated with TLR ligands and ODN/peptide complexes for 6 hours and RNAs were isolated, converted into cDNA and PCR was performed for Mx transcript detection using specific primers. Figure 3.11 shows the gel image of the PCR products and the results indicate that K23/Tat retained its Mx transcript inducing activity whereas LL37 was less effective when compared to free K23.

Figure 3.11. Agarose gel images of Mx PCR products. Splenocytes were stimulated with 1 μM ODN and ODN/peptide complexes and the TLR ligands for 6 hours. 25 μl of sample product was loaded per well with 5 μl of loading dye (6X). Samples were run on a 1% agarose gel with 10 mg/ml EtBr at 60V for 1 hour. Product size was 485 base pairs and was confirmed using a 1kb ladder.

Next, IFNγ production was determined by ELISA following 24 hours of stimulation with three different doses (0.3, 1 and 3 μM) of the optimum complex molar ratios determined in human studies. The results given in Figure 3.12 show that K23/Tat was the most effective formulation, triggering significantly higher levels of IFNγ ($P<0.05$) even when used at the lowest dose (0.3 μM; 6-fold more IFNγ when compared to free ODN).

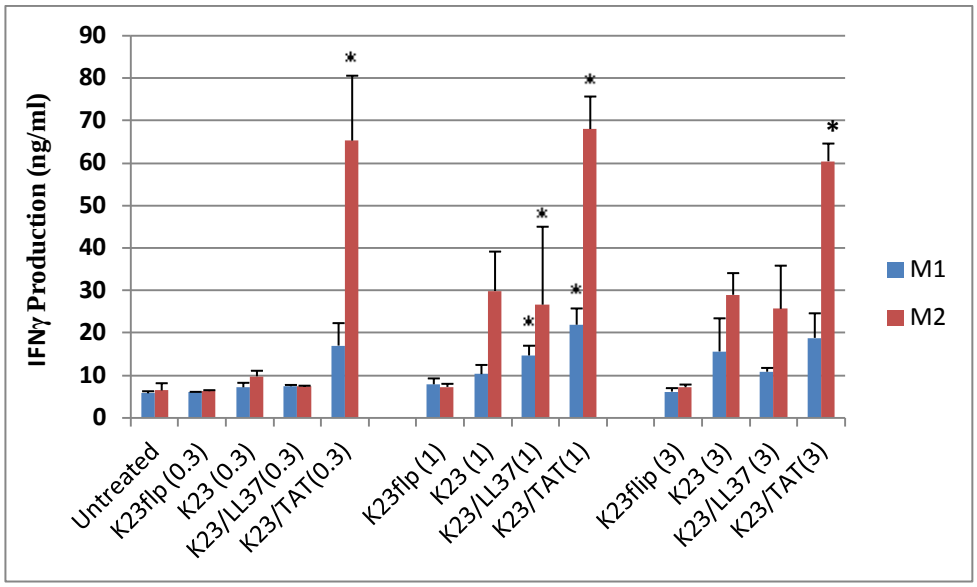

Figure 3.12 IFNγ production from mouse splenocytes following stimulation with three different doses (0.3, 1 and 3μM) of K23, K23/LL37 (1:8) and K23/TAT (1:16). The results are average of 2 duplicate well ± S.D. All labeled groups were compared with the same dose of free K23 and * indicates $P<0.05$.

3.3. Analysis of Cell-Surface Binding and Internalization of Complexes

In the first part of the study, CAL-1 cells were stimulated with FAM labeled K3 ODN alone or its complexes with the peptides and K3-FAM positive cells were analyzed (this signal is a combination of cell surface-bound and internalized ODN signal and hence will be called as "cell-associated total fluorescence". In the second part of the study, same cells were subjected to trypan blue quenching which enabled the detection of only the internalized K3-FAM signal but not the cell-surface associated signal. A representative experiment showing the percentages of total fluorescent ODN associated with the cells prior to and following trypan blue addition is given in Figure 3.13.

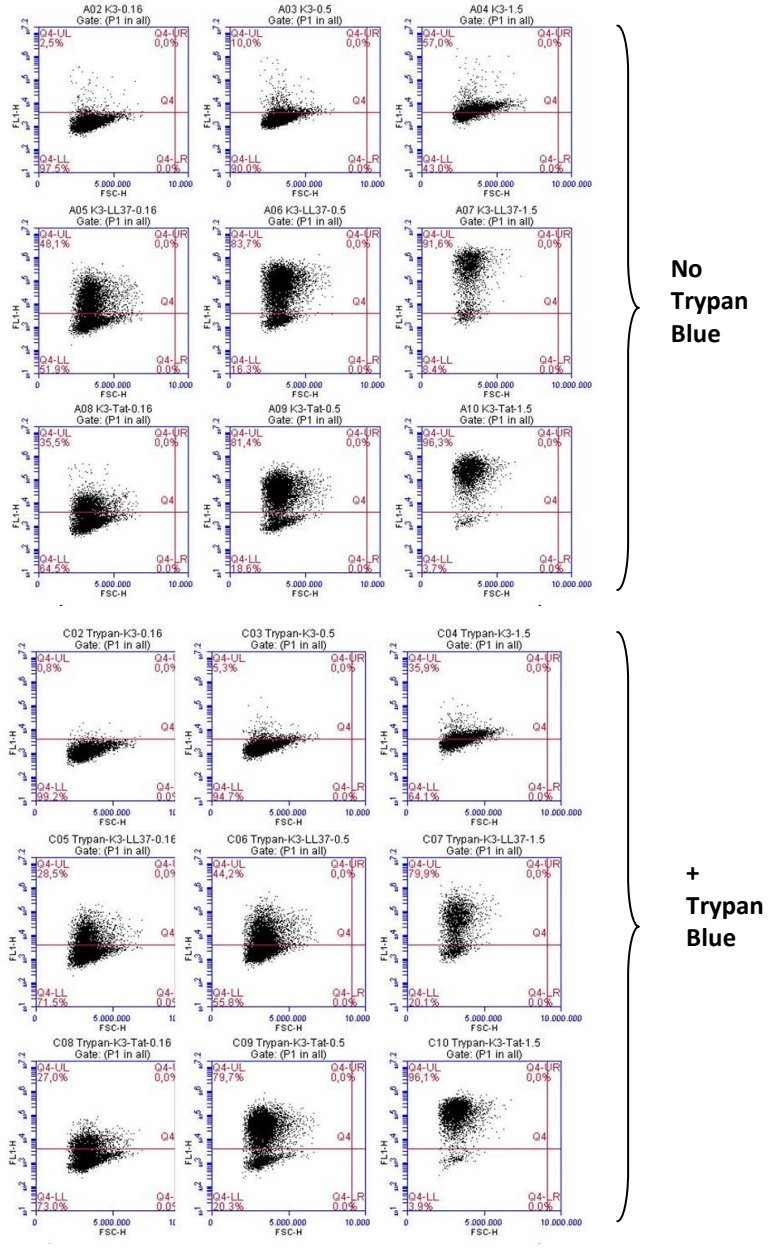

Figure 3.13 Percentages of K3-FAM positive cells before and after quenching of the cell surface-bound signal by trypan blue. FAM labeled CpG ODN/peptide complexes (0.16, 0.5 and 1.5 μM) were incubated with CAL-1 cells (400,000 cells/well) in a total volume of 200 μl for 1 h at 37°C. Following washing, FAM-ODN positive cells were detected by flow cytometry prior to and following trypan blue addition (equal volume addition of 1:10 diluted dye).

The results from three independent experiments are summarized in Figure 3.14. Data show that, for all groups, ODN binding and uptake increased in a concentration dependent manner (Figure 3.14, blue bars). Moreover, complexation with both LL37 and TAT peptide enhanced the binding and uptake of the ODN. Of note, the binding/uptake of 0.5 µM CpG ODN/peptide complexes exceeded that of 1.5 µM free ODN, suggesting that peptide complexation masked the negative charge density of the ODN, enhancing cellular interaction (P<0.004 for LL37 and P<0.06 for TAT ODN; blue bars).

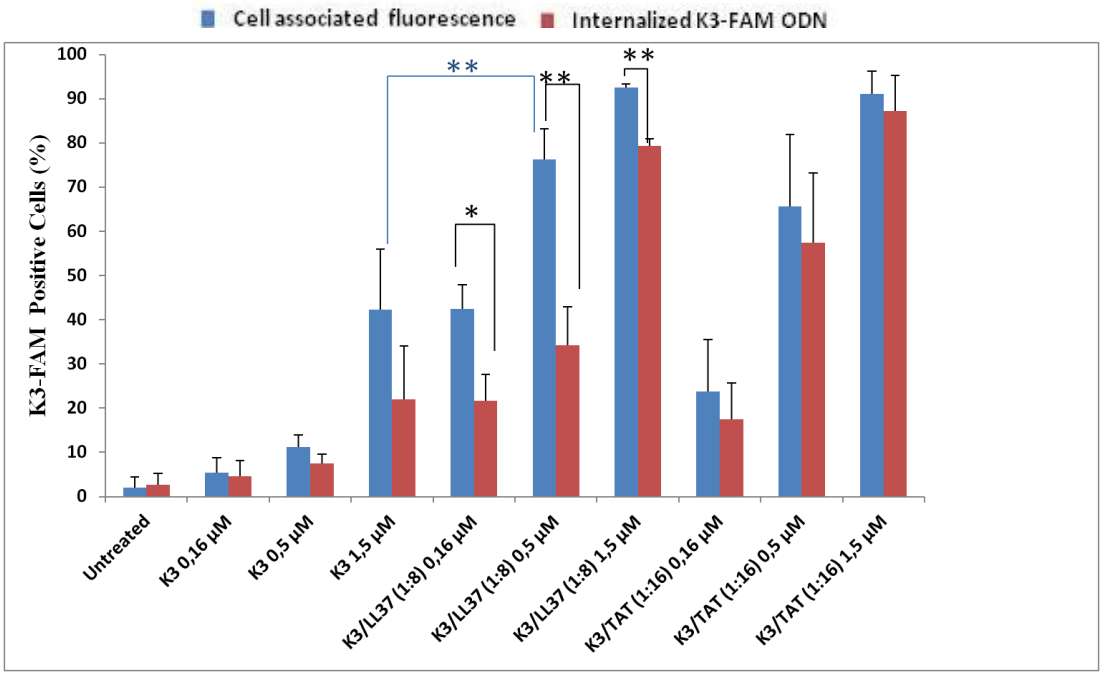

Figure 3.14 Total cell associated fluorescence (blue bars; unquenched) and internalized K3-FAM ODN (red bars; trypan blue quenched) as such or following complexation with LL37 or TAT peptides. Results are average of 3 independent experiments ± S.D. Percentages of K3-FAM positive cells were determined on a flow cytometer as described in Figure 3.6 (** P< 0.005; * P< 0.01).

The results showed that, all of the complexes with the TAT peptide were internalized by the cells ($P<0.05$ for all concentrations of K3/TAT complexes; red bars) whereas for the LL37/CpG ODN complexes, only half of the total cell-associated fluorescence derived from the internalized fraction indicating that the hydrophobic residues of the LL37 peptide localized 50 % of the complex to the plasma membrane (compare the blue vs the red bars; $P<0.005$ for 0.5 μM and $p<0.01$ for 1.5 μM K3/LL37 complex with respect to : cell associated fluorescence and internalized K3-FAM ODN).

3.4. Determination of Nuclease Resistance of Complexes Following DNAse Treatment

Upon *in vivo* administration, CpG oligodeoxynucleotide-based therapeutic agents are susceptible to nuclease attack, reducing their immunostimulatory potential. Since complexation with cationic peptides can protect against such nuclease digestion and improve the stability of the ODN, CpG ODN containing complexes were first exposed to DNAse I followed by stimulation of human PBMCs as described before. DNAse untreated complexes were also used for comparison. As expected, all samples that were not treated with DNAse I stimulated IP-10 production from human PBMC (Figure 3.15 (A), red bars). In contrast, following DNAse I treatment, K23/LL37 complex retained only 40% of its activity ($p< 0.05$ with respect to the untreated sample; blue bars) whereas approximately 80 % of the immunostimulatory activity of K23/TAT complex was still intact ($p < 0.05$; blue bars). A detailed analysis of nuclease resistance following complexation with increasing molar ratios of Tat peptide was also undertaken and is presented in Figure 3.15 (B). Consistent with the particle stability data, a lower ratio of CpG:Tat (1:8) was also capable of protecting the ODN from DNase digestion (~ 70% of protected activity). It was concluded that TAT complexes were more resistant to DNAse digestion than LL37 complexes.

A

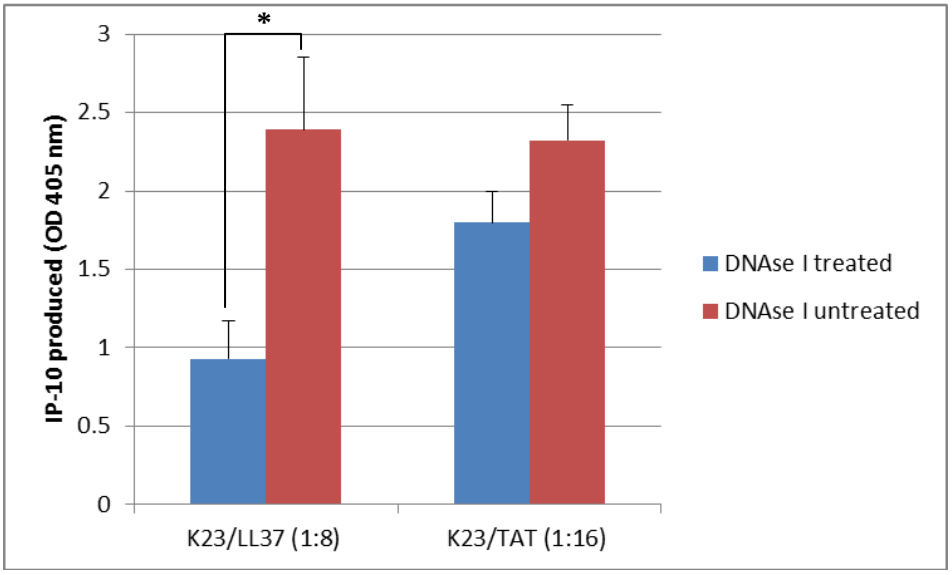

B

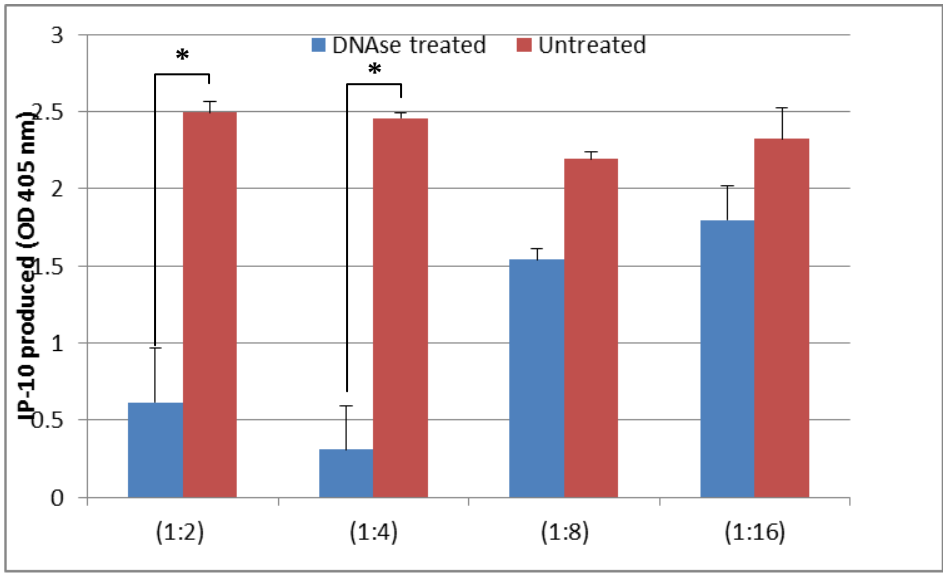

Figure 3.15 IP-10 production from human PBMCs stimulated with DNAse I pre-treated or untreated K23/LL37 and K23/TAT complexes. Complexes were treated with of 1.1 U of DNAse I/µg of ODN for 10 min at 37°C (A). Cells were then stimulated with DNAse I treated and untreated complexes (1 µM) for 24 h and IP-10 production was assessed from culture supernatants by ELISA (B). Results show the IP-10 production from 3 different PBMCs± S.D. (* indicates $P< 0.05$).

3.5. Cell Viability Assay

Some cationic peptides are known to cause cytotoxicity. Therefore the possible cytotoxicities of the complexes were tested using Propidium Iodide (PI) staining. The cell membrane is not permeable to PI and it is excluded from viable cells. Therefore, PI is commonly used to identify dead cells in a population. Two different cell lines were treated with the complexes for a period of 24 h prior to PI staining. Untreated cells were used as the negative control. Approximately 15 % of CAL-1 cells and 10 % of RAW cells were dead at the end of 24 hours incubation (untreated cells). For both cell types tested, the complexes showed no significant increase in the number of PI positive dead cells when compared to their untreated controls (Figure 3.16) indicating that the K23/LL37 and K23/TAT complexes are not toxic for the human and mouse cells.

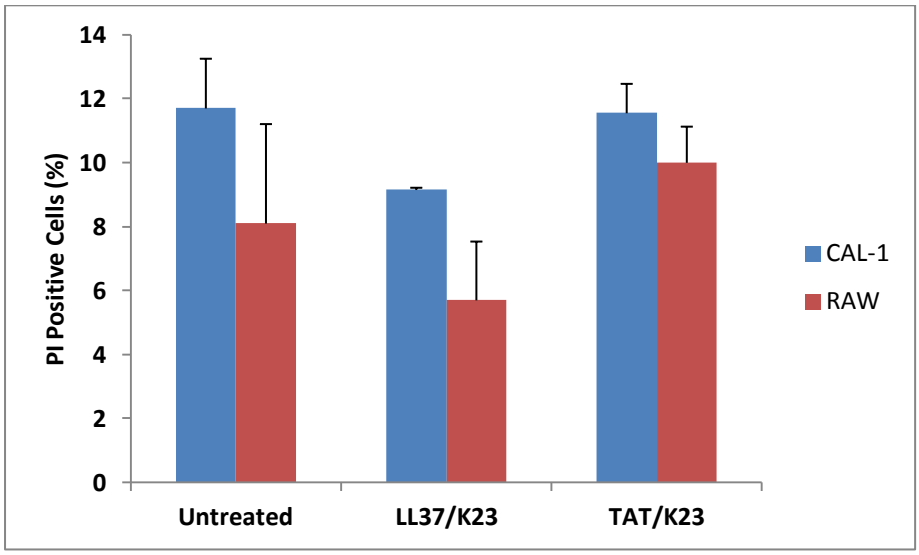

Figure 3.16 Percentage of PI positive dead following 24 h incubation with complexes. CAL-1 and RAW cells were treated for 24 h with 1 μM of complexes and stained with 0.2 μg/ml of PI prior to analysis on a flow cytometer. Results are the average of two independent experiments ± S.D.

3.6. Determination of Subcellular Distribution of CpG ODN/peptide Complexes by Confocal Microscopy

Previous studies showed that subcellular distribution of internalized CpG ODN affects its immunostimulatory activity (Gursel, 2006). Moreover, different classes of CpG ODN were shown to localize to different subcellular compartments, activating a different signal transduction pathway. To determine whether complexation changed the subcellular localization and thus the immunostimulatory property of the CpG ODN, colocalization studies were performed. K type CpG is known to localize to lysosomal vesicles that are labeled with the LysoTracker dyes but not with the transferrin positive early endosomes. Similar to earlier findings, K3-FAM did not colocalize with transferrin-Texas Red (absence of yellow signal; Figure M-A) indicating that K3-Cy5 was not present in early endosomes. In contrast, K3/LL37 and K3/TAT complexes showed colocalization with transferrin (Figure 3.18 (A)), middle and lower panels) which was more extensive for the latter complex, suggesting that complexation with cationic peptides targets the CpG ODN to early endosomes. Confocal analysis of cells stained with LysoTracker marker also confirmed that the complexes were excluded from the lysosomal compartment (Figure 3.18 (B)). In conclusion, unlike the free CpG ODN, the complexes mainly localized to early endosomes. Consequently, complexation with peptides changes the subcellular distribution of the CpG ODN, initiating a different signal transduction pathway favoring type I interferon production.

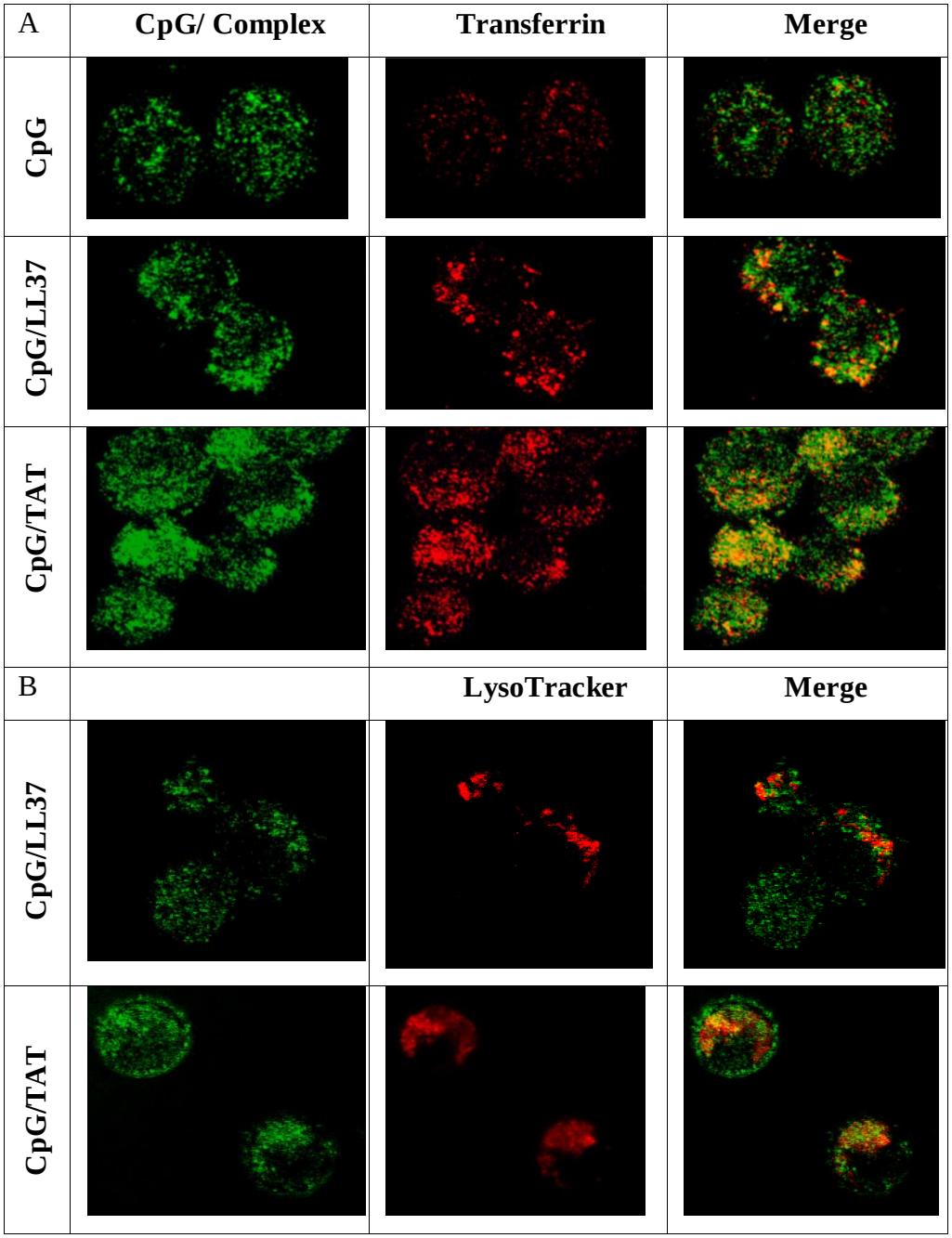

Figure 3.17 Subcellular distribution of CpG ODN/peptide complexes. RAW cells were incubated with Cy5 conjugated CpG ODN (1 μM) or its complexes in the presence of 75 nM of LysoTracker Red (marker for lysosomal compartment) or 25 μg/ml Transferrin-texas red conjugate (marker for early/recycling endosomes). A. Colocalization of free CpG-Cy5 and its peptide complexes with transferrin-texas red. B. Colocalization of complexes with LysoTracker Red.

3.7 Vaccination Studies

The aim of the vaccination studies was to potentiate the immunostimulatory activity of CpG ODN by simple complexation with the cell penetrating peptide Tat to generate a potent adjuvant formulation that specifically increase the precursor frequency of IgG_{2a} secreting cells in mice immunized with the inactivated foot and mouth disease (FMD) vaccine.

3.7.1 Antibody Mediated Immune Response

Antibody mediated responses are produced by B lymphocytes. The antibodies neutralize toxins, block adhesion and cell entry of microorganisms, prevent viral replication or eliminate pathogens through complement-mediated killing. When a B cell encounters an antigen, it is stimulated to proliferate and starts secreting antibodies specific to that antigen (MacLannen, 2003). During differentiation of B cells, they switch the class of immunoglobulins they produce (from IgM to IgG, IgA or IgE). This process is guided by helper T cells. Mice have four different classes of IgGs, named IgG1, IgG2a, IgG2b and IgG3. Antiviral antibodies elicited by infection belong to the IgG2a subclass, which depend on Th_1 type of helper T cells for their production. In contrast, antibodies against soluble proteins or carbohydrates are restricted to IgG1 and IgG3 subclasses that are dependent on Th_2 cells (Banerjee, 2010). Therefore, a good anti-viral response is achieved via Th_1 dominated immunity and the ratio of IgG2a and IgG1 levels is a useful parameter to examine the success of the vaccines designed against viral infections.

3.7.1.1. Determination of Antigen specific IgG1 and IgG2a antibodies by ELISA

6-8 week old female BALB/c mice (5/group) were immunized on days 0, 15 and 180 as explained in Section 2.2.10.2. Two weeks after each injection, sera were collected and IgG1 and IgG2a levels were detected by ELISA. Two weeks after the first injection (the primary response) all vaccinated groups had detectable levels of antigen specific IgG2a and IgG1 (Figure 3.18). The ratio of IgG2a over IgG1 (an indicator of antiviral response) was 4 times higher in animals immunized with CpG ODN/Tat adjuvanted FMD vaccine when compared to FMDV vaccinated group ($P<0.05$, Figure 19). This trend was maintained during the secondary response and was calculated to be 3 times higher than the FMDV vaccinated animals. Use of low dose CpG ODN or its LL37 complexed form as an adjuvant was not significantly different than the FMDV immunized groups (Figure 3.18). In conclusion, CpG ODN/Tat was the only adjuvant formulation capable of enhancing the Th_1 type of immune response, consistent with the outcome of in vitro stimulation experiments in mice.

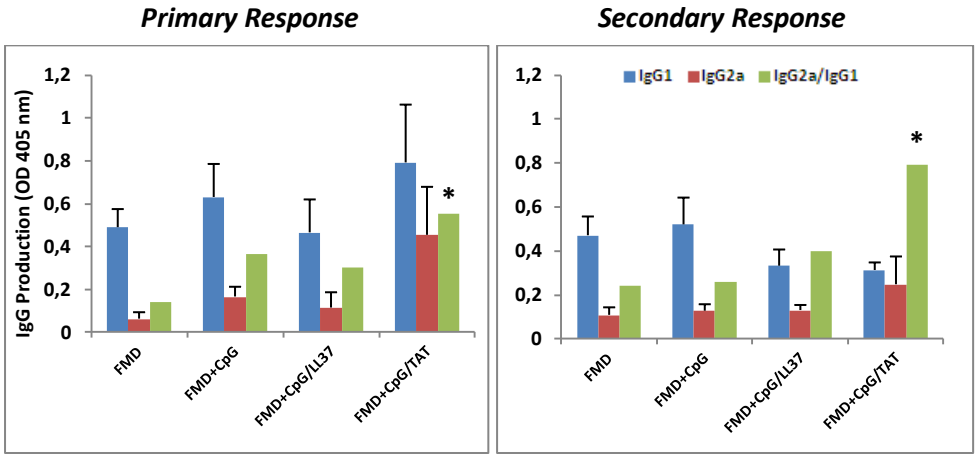

Figure 3.18. Primary and secondary responses showing FMDV specific IgG1 and IgG2a titers. Graphs show the absorbance readings at 400X and 2800X titrated sera for primary response and secondary response, respectively. Green bars show the corresponding IgG2a/IgG1 ratios. The results are the average of 5 mice ± S.D. * indicates statistically significant difference ($P<0.05$).

3.7.1.2. Determination of IgG Secreting Cell Frequency and assessment of long-term immunity

The frequencies of serotype O specific IgG_1 or IgG_{2a} secreting cells were determined using a limiting dilution assay following boosting of animals six months after the first injection. This long-term follow up was a necessary part of the study since IgG secreting cells can only be detected if the prior two immunizations were capable of generating long lasting memory B cells. Dose response data was analyzed according to the Poisson single-hit model, which assumes that the number of biologically active particles in each culture varies according to a Poisson distribution, and states that when 37% of the test culture is negative, there is an average of 1 precursor cell that is responding (Greenwood and Yule, 1917; Taswell, 1981). In short, of all the wells from one group of mice, % of nonresponding wells were calculated and this value was plotted against the corresponding cell concentration. The best-fitted linear lines that intercepted the numeric value of 0.37 (corresponds to 37%), gave us the frequency of antigen-specific IgG1 or IgG2a producers. The fraction of antigen-specific IgG1 and IgG2a responders are shown in Figure 3.19.

Briefly, results show that IgG1 secreting cell frequencies of animals immunized with the FMD vaccine adjuvanted with CpG, CpG/LL-37 and CpG/Tat were determined to be 1/30,000, 1/110,000 and 1/100,000, respectively, whereas the frequencies of IgG_{2a} secreting cells were 1/88,000, 1/52,000 and 1/12,000, indicating that CpG/Tat preferentially expanded the population of IgG_{2a} secreting cells. In summary, CpG ODN preferentially stimulated FMDV specific IgG1 secreting cells whereas CpG ODN/Tat complex induced 7X more ($P<0.05$) antigen specific IgG2a secreting cells compared to CpG ODN adjuvanted groups. Moreover, these results also demonstrate that CpG/Tat can provide long-lasting immunity against FMD, suggesting an efficient mechanism of memory B cell formation.

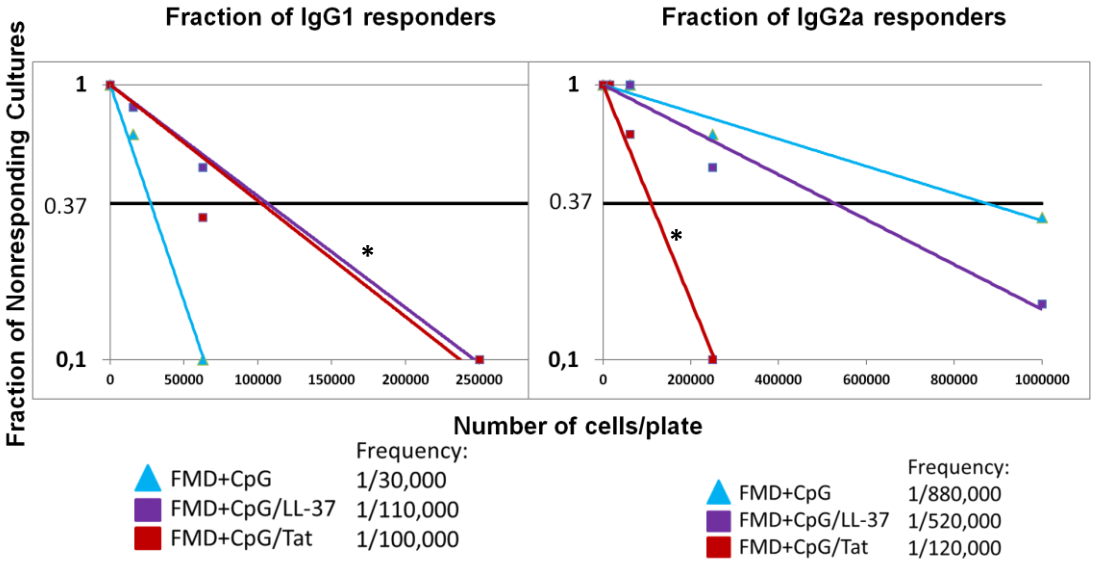

Figure 3.19 Limiting dilution analysis 6 months after the initial immunization. Splenocytes were cultured on antigen coated plates for 24 h and the levels of specific IgG1 and IgG2a were assessed colorimetrically. The results show the average of 3 mice ± S.D. * indicates statistically significant difference ($P<0.05$).

3.7.2 Cell Mediated Immune Response

Cell mediated immunity is controlled by T lymphocytes. CD4+ T cell activation by DCs triggers their differentiation into distinct pathways. Th1-type CD4+ T cells essentially contribute to the elimination of intracellular pathogens through the cytokines they produce (for eg., IFN-γ) and by supporting macrophage activation and CD8+ T cell (cytotoxic T cells) differentiation. Cytotoxic T cells recognize and destroy infected cells and activate phagocytes to destroy pathogens that they have internalized (O'Garra, 2004).

3.7.2.1 Detection of Antigen Specific IFNγ Production by ELISA

IFNγ is the hallmark cytokine secreted from Th1 cells and CD8+ cytotoxic T cells. Thus, its production is used as an indicator of cellular immune response. 6 months

following the first injection, animals were vaccinated as described above and 24 h later, the amount of circulating IFNγ was assessed from sera by ELISA. As shown in Figure 3.20, the group that received CpG ODN/TAT adjuvanted vaccine had the highest levels of IFNγ among the immunized groups, which was twofold more than the FMD vaccinated group ($P<0.05$). The group adjuvanted with CpG ODN /LL37 complex on the other hand, showed no statistically significant difference from the group vaccinated with FMD.

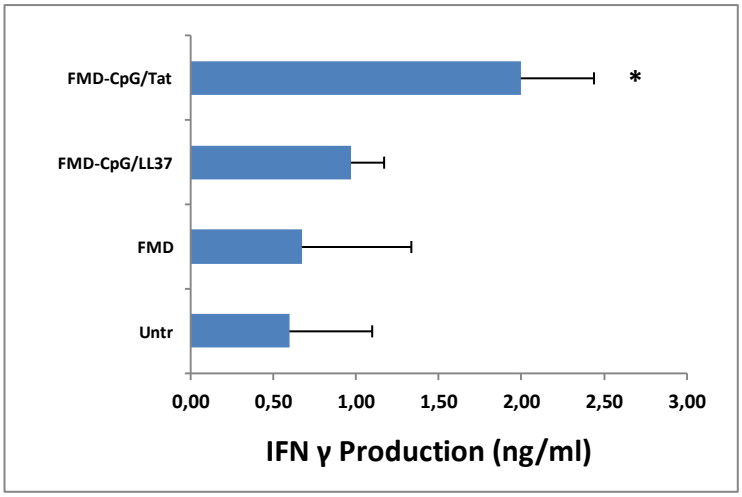

Figure 3.20 Circulating levels of IFNγ in sera of mice immunized 6 months after the first vaccination. Sera were collected 24 h after the immunization and cytokine levels were assessed by ELISA. The results show the average of 5 mice ± S.D. * indicates statistically significant difference ($P<0.05$). Amounts of IFNγ produced by CpG ODN/TAT adjuvanted group is two folds more in comparison to the group vaccinated with FMD only.

These results suggest that CpG ODN/Tat complex was able to trigger Th_1 mediated antiviral response and provided help for the production of FMD specific IgG2a antibodies. Furthermore, this formulation led to sustained humoral (antibody mediated) immunity and IFNγ mediated cellular immunity even 6 months after the initial immunization.

CHAPTER 4

CONCLUSION

The present study demonstrated that complexation of the conventional K-type CpG ODN with cationic peptides modified its immunostimulatory properties and switched its Class towards an IFNα-inducing one. This activity strongly correlated with stable nanoparticle formation as evidenced by the zeta potentials and particle size analysis studies. Among the tested cationic peptides (KR-12, LL37 and Tat), the HIV derived Tat peptide formed the most stable nanoparticles when used at a molar ratio of 1:16 and stimulated large amounts of IFNα in human PBMC when used at the optimum concentration of 1 μM. Complexation resulted in increased nuclease resistance. Confocal studies confirmed that in contrast to conventional K-ODN, the complexes localized to transferrin positive early endosomes and not to lysosomes. This pattern of subcellular distribution is mandatory for IFNα production. Our studies also confirmed that unlike D-type ODN, the complexes could still stimulate TNFα from pDCs, a cytokine that further contributes to the activation of NK cells and cytotoxic T cells. *In vivo*, Tat containing K-ODN complexes were found to be the most effective vaccine adjuvant in inducing long-term FMDV specific immunity. This formulation also increased the circulating serum IFNγ levels in mouse within 24 h of its administration, further supporting induction of a Th1-specific immune response. Collectively, these results show that the combination of K-ODN/Tat modifies and potentiates the CpG ODN's immunostimulatory activity and could impact the field of innate immunity, leading to the general use of these complexes as vaccine adjuvants and anti-viral therapeutic agents.

REFERENCES

Akira S, Uematsu S, Takeuchi O. (2006). *Pathogen recognition and innate immunity*. Cell. 124(4):783–801.

Alexopoulou, L., Holt A. C., (2001). *Recognition of double-stranded RNA and activation of NF-kappaB by Toll-like receptor 3*. Nature 413(6857): 732-8.

Alves, D., and Fontanari J. F. (1998). *Error threshold in finite populations*. Phys. Rev. E 57:7008–7013.

Asselin-Paturel C, Brizard G, Chemin K, *et al*. (2005). *Type I interferon dependence of plasmacytoid dendritic cell activation and migration*. J Exp Med. 201(7):1157–1167.

Bagchi, A., Herrup E. A., (2007). *MyD88-dependent and MyD88-independent pathways in synergy, priming, and tolerance between TLR agonists.* J Immunol 178(2): 1164-71.

Bal, S. M., Hortensius S., *et al*. (2011) *Co-encapsulation of antigen and Toll-like receptor ligand in cationic liposomes affects the quality of the immune response in mice after intradermal vaccination*. Vaccine 29(5): 1045-52.

Banerjee K, Klasse PJ, Sanders RW, Pereyra F, Michael E, Lu M, Walker BD, Moore JP. (2010). *IgG subclass profiles in infected HIV type 1 controllers and chronic progressors and in uninfected recipients of Env vaccines.* AIDS Res Hum Retroviruses, 26:445-458.

Bernasconi NL, Traggiai E, Lanzavecchia A. (2002) *Maintenance of serological memory by polyclonal activation of human memory B cells*. Science. 298(5601):2199–2202.

Bernasconi NL, Traggiai E, Lanzavecchia A. (2002) *Maintenance of serological memory by polyclonal activation of human memory B cells*. Science, 298(5601):2199-202.

Blackwell SE, Krieg AM. (2003). *CpG-A-induced monocyte IFN-gammainducible protein-10 production is regulated by plasmacytoid dendritic cell-derived IFN-alpha*. J Immunol. 170(8):4061–4068.

Blasius, A. L. and Beutler B. (2010). *Intracellular toll-like receptors*. Immunity 32(3): 305-15.

Bode, C., Zhao G., *et al*. (2011). *CpG DNA as a vaccine adjuvant*. Expert Rev Vaccines 10(4): 499-511.

Cao W, Liu YJ. (2007) *Innate immune functions of plasmacytoid dendritic cells.* Current Opinion in Immunology, 19(1):24-30.

Carrillo C, Tulman ER, Delhon G, (2005). Comparative Genomics of Foot and Mouth Disease Virus. *J. Virol*. 79 (10): 6487–504. doi:10.1128/JVI.79.10.6487-6504.2005.

Cervantes-Barragan, L., Lewis K. L., *et al*. (2012). *Plasmacytoid dendritic cells control T-cell response to chronic viral infection.* Proc Natl Acad Sci U S A 109(8): 3012-7.

Chen ZJ. (2005) *Ubiquitin signalling in the NF-kappaB pathway*. Nat Cell Biol 7:758–65.

Chuang CM Monie A, Wu A, Mao CP, Hung CF,. (2009). *Treatment with LL-37 peptide enhances antitumor effects induced by CpG oligodeoxynucleotides against ovarian cancer*. Hum. Gene. Ther., 20(4), 303-13.

Costa LT, Kerkmann M, Hartmann G, Endres S, Bisch PM, Heckl WM, Thalhammer S. (2004) *Structural studies of oligonucleotides containing G-quadruplex motifs using AFM. Biochemical and Biophysical Research Communication.*, 313(4):1065-72.

Cristina D. C., Thorgerdur S., *et al*. (2005) *Antimicrobial and Chemoattractant Activity, Lipopolysaccharide Neutralization, Cytotoxicity, and Inhibition by Serum of Analogs of Human Cathelicidin LL-37*. Antimicrob Agents Chemother.; 49(7): 2845–2850.

Degn, S. E., Thiel S., *et al*. (2007). *New perspectives on mannan-binding lectin-mediated complement activation.* Immunobiology 212(4-5): 301-11.

Diaz-San, F., Weiss M., (2011) *Antiviral activity of bovine type III interferon against foot-and-mouth disease virus.* Virology 413(2): 283-92.

Diebold S.S., Kaisho T., Hemmi H., Akira S., Reis E., and Sousa C. (2004). *Innate antiviral responses by means of TLR7-mediated recognition of single-stranded RNA.* Science 303, 1529–1531.

Doel TR. *FMD vaccines.* Virus Research (2003) 91(1):81–99.

Domenech, J., Lubroth J., *et al*. *Immune Protection in Animals: The Examples of Rinderpest and Foot-and-Mouth Disease*. Journal of Comparative Pathology 142, Supplement 1(0): S120-S124.

Doyle, S., Vaidya S., *et al*. (2002). *IRF3 mediates a TLR3/TLR4-specific antiviral gene program*. Immunity 17(3): 251-63.

Endres, A.M. Krieg, Hartmann G., (2001). *Identification of CpG oligonucleotide sequences with high induction of IFN-alpha/beta in plasmacytoid dendritic cells*, Eur. J. Immunol. 31 2154–2163.

Fitzgerald KA, McWhirter SM, Faia KL, Rowe DC, Latz E, Golenbock DT, (2003). *IKKepsilon and TBK1 are essential components of the IRF3 signaling pathway*. Nat Immunol 4:491–6.

Gilliet, M., Cao W., *et al*. (2008). *Plasmacytoid dendritic cells: sensing nucleic acids in viral infection and autoimmune diseases.* Nat Rev Immunol 8(8): 594-606.

Golde WT, Pacheco JM, Duque H, Doel T, Penfold B, Ferman GS, (2005) *Vaccination against foot-and-mouth disease virus confers complete clinical protection in 7 days and partial protection in 4 days: use in emergency outbreak response.* Vaccine 2005 23(50):5775–82.

Gray RC, Kuchtey J, Harding CV. (2007) *CpG-B ODNs potently induce low levels of IFN-alphabeta and induce IFN-alphabeta-dependent MHC-I cross-presentation in DCs as effectively as CpG-A and CpG-C ODNs.* J Leukoc Biol.; 81(4):1075-85.

Greenwood, M., and Yule, G.U. (1917) *On the statistical interpretation of some bacteriological methods employed in water analysis*. J. Hyg., 16, 36-54

Grubman MJ., Baxt B., (2004). *Foot-and-mouth disease*. Clinical Microbiology Reviews (2):465–93.

Gursel M, Verthelyi D, Gürsel I, Ishii KJ, Klinman DM. (2002). *Differential and competitive activation of human immune cells by distinct classes of CpG oligonucleotide.* J Leukoc Biol. 71(5):813–820.

Gursel, M., I. Gursel, (2006). *CXCL16 influences the nature and specificity of CpG-induced immune activation*. J Immunol 177(3): 1575-80.

Hanagata, N. (2012). *Structure-dependent immunostimulatory effect of CpG oligodeoxynucleotides and their delivery system.* Int J Nanomedicine 7: 2181-95.

Hartmann G, Battiany J, Poeck H, Wagner M, Kerkmann M, Lubenow N, Rothenfusser S, Endres S. (2003) *Rational design of new CpG oligonucleotides that combine B cell*

activation with high IFN-alpha induction in plasmacytoid dendritic cells. European Journal of Immunology, 33(6):1633-41.

Heeg, K., A. Dalpke, *et al*. (2008). *Structural requirements for uptake and recognition of CpG oligonucleotides.* Int J Med Microbiol 298(1-2): 33-8.

Heil F., Hemmi H., Hochrein H., Ampenberger F., Kirschning C., Akira S., Lipford G., Wagner H., and Bauer S. (2004). *Species-specific recognition of single-stranded RNA via toll-like receptor 7 and 8.* Science 303, 1526–1529

Hemmi, H., Takeuchi O., *et al.* (2000). *A Toll-like receptor recognizes bacterial DNA*. Nature 408(6813): 740-5.

Hiroshima, Y., Bando M., *et al*. (2012). *Regulation of antimicrobial peptide expression in human gingival keratinocytes by interleukin-1alpha.* Arch Oral Biol 56(8): 761-7.

Hu Y, Jin H, Du X, Xiao C, Luo D, Wang B, She R. (2007). *Effects of chronic heat stress on immune responses of the foot-and-mouth disease DNA vaccination.* DNA Cell Biol 26(8):619-26.

Hoebe K, Du X, Georgel P, Janssen E, Tabeta K, Kim SO, et al. (2003) *Identification of Lps2 as a key transducer of MyD88-independent TIR signalling.* Nature 424:743–8.

Hollmig, S. T., Ariizumi K., *et al.* (2009). *Recognition of non-self-polysaccharides by C-type lectin receptors dectin-1 and dectin-2.* Glycobiology 19(6): 568-75.

Honda K, Ohba Y, Yanai H, Negishi H, Mizutani T, Takaoka A, Taya C, Taniguchi T. (2005) *Spatiotemporal regulation of MyD88-IRF-7 signaling for robust type-I interferon induction.* Nature, 434(7036):1035-40.

Hoshino, K., Kaisho T., *et al*. (2002). *Differential involvement of IFN-beta in Toll-like receptor-stimulated dendritic cell activation*. Int Immunol 14(10): 1225-31

Hurtado P. and Peh C. A., (2010) *LL-37 Promotes Rapid Sensing of CpG Oligodeoxynucleotides by B Lymphocytes and Plasmacytoid Dendritic Cells* J Immunol 184:1425-1435

Ito T., Amakawa R., Kaisho T., Hemmi H., Tajima K., Uehira K., Ozaki Y., Tomizawa H., Akira S., and Fukuhara S. (2002). *Interferon-alpha and interleukin-12 are induced differentially by Toll-like receptor 7 ligands in human blood dendritic cell subsets*. J. Exp. Med. 195, 1507–1512

Jahrsdörfer, B., Hartmann G., *et al.* (2001). *CpG DNA increases primary malignant B cell expression of costimulatory molecules and target antigens.* Journal of Leukocyte Biology 69(1): 81-88.

Janeway, C. A., Jr. and Medzhitov R. (2002). *Innate immune recognition*. Annu Rev Immunol 20: 197-216

Jung J, Yi AK, Zhang X, Choe J, Li L, Choi YS. (2002). *Distinct response of human B cell subpopulations in recognition of an innate immune signal, CpG DNA.* J Immunol. 169(5):2368–2373.

Jurk, M., Heil, F., Vollmer, J., Schetter, C., Krieg, A.M., Wagner, H., Lipford, G., and Bauer, S. (2002). *Human TLR7 or TLR8 independently confer responsiveness to the antiviral compound R-848*. Nat. Immunol. 3, 196–200.

Jurk, M., Schulte B., *et al.* (2004). *C-Class CpG ODN: sequence requirements and characterization of immunostimulatory activities on mRNA level*. Immunobiology 209(1-2): 141-54.

Kaisho, T. and Akira S. (2001). *Toll-like Receptors.* eLS, John Wiley & Sons, Ltd.

Kawai, T. and Akira S. (2010). *The role of pattern-recognition receptors in innate immunity: update on Toll-like receptors*. Nat Immunol 11(5): 373-84.

Kawai, T. and Akira S. (2009). *The roles of TLRs, RLRs and NLRs in pathogen recognition*. Int Immunol 21(4): 317-37.

Kawai, T. and Akira S. (2007). *Signaling to NF-kappaB by Toll-like receptors.* Trends Mol Med 13(11): 460-9.

Kawai, T. and Akira S. (2007). *TLR signaling.* Semin Immunol 19(1): 24-32.

Kenny, E. F. and O'Neill L. A. J. (2008). *Signalling adaptors used by Toll-like receptors: An update.* Cytokine 43(3): 342-349.

Kerkmann M, Costa LT, Richter C, *et al.* (2005). *Spontaneous formation of nucleic acid-based nanoparticles is responsible for high interferon-alpha induction by CpG-A in plasmacytoid dendritic cells.* J Biol Chem. 280(9):8086–8093.

Kis-Toth, K., Szanto A., *et al.* (2011) *Cytosolic DNA-activated human dendritic cells are potent activators of the adaptive immune response.* J Immunol 187(3): 1222-34.

Klein DC, Latz E, Espevik T, Stokke BT. (2010). *Higher order structure of short immunostimulatory oligonucleotides studied by atomic force microscopy.* Ultramicroscopy. 110(6):689–693.

Klinman, D. M., Klaschik S., *et al*. (2009). *CpG oligonucleotides as adjuvants for vaccines targeting infectious diseases.* Adv Drug Deliv Rev 61(3): 248-55.

Klinman D.M., Xie H. And Ivins B. E. (2006). *CpG oligonucleotides improve the protective immune response induced by the licensed anthrax vaccine*. Annals of the New York Academy of Sciences. 1082:137 150.

Klinman, D. M. (2004). *Immunotherapeutic uses of CpG oligodeoxynucleotides.*Nat Rev Immunol 4(4): 249-58.

Krieg AM. (2006) *Therapeutic potential of Toll-like receptor 9 activation.* Nature Reviews Drug Discovery, 5(6):471-84.

Krieg, A. M., Yi A.-K., *et al*. (1995*). CpG motifs in bacterial DNA trigger direct B-cell activation.* Nature 374(6522): 546-549.

Krug A, Rothenfusser S, Hornung V, Jahrsdörfer B, Blackwell S, Ballas ZK, Endres S, Krieg AM, Hartmann G.(2001) *Identification of CpG oligonucleotide sequences with high induction of IFN-alpha/beta in plasmacytoid dendritic cells.* European Journal of Immunology, 31(7): 2154-63.

Kucera, K., Koblansky A. A. (2010). *Structure-Based Analysis of Toxoplasma gondii Profilin: A Parasite-Specific Motif Is Required for Recognition by Toll-Like Receptor 11*. Journal of Molecular Biology 403(4): 616-629.

Kumagai Y, Takeuchi O, Akira S. (2008) *TLR9 as a key receptor for the recognition of DNA.* Advanced Drug Delivery Reviews, 60(7):795-804.

Kumar, H., Kawai T., *et al*. (2009). *Toll-like receptors and innate immunity*. Biochem Biophys Res Commun 388(4): 621-5.

Lagging, M., Romero A. I., *et al.* (2006). *IP-10 predicts viral response and therapeutic outcome in difficult-to-treat patients with HCV genotype 1 infection*. Hepatology 44(6): 1617-1625.

Lande, R., Gregorio J., *et al*. (2007). *Plasmacytoid dendritic cells sense self-DNA coupled with antimicrobial peptide*. Nature 449(7162): 564-9.

Lechmann, M., Zinser E., *et al.* (2002). *Role of CD83 in the immunomodulation of dendritic cells.* Int Arch Allergy Immunol 129(2): 113-8.

Leifer CA, Verthelyi D, Klinman DM. (2003). *Heterogeneity in the human response to immunostimulatory CpG oligodeoxynucleotides*. Journal of Immunotherapy, 26(4):313-9.

Li J, Pei H, Zhu B, *et al. Self-assembled multivalent DNA nanostructures for noninvasive intracellular delivery of immunostimulatory CpG oligonucleotides.* ACS Nano. 2011;5(11):8783–8789.

Lievin-Le Moal, V. and Servin A. L. (2006). *The Front Line of Enteric Host Defense against Unwelcome Intrusion of Harmful Microorganisms: Mucins, Antimicrobial Peptides, and Microbiota*. Clinical Microbiology Reviews 19(2): 315-337.

Litman G., Cannon J., Dishaw L. (2005). *Reconstructing immune phylogeny: new perspectives.* Nat Rev Immunol 5 (11), 866-79.

Liu, Y., Luo X., *et al*. (2011). *Three CpG oligodeoxynucleotide classes differentially enhance antigen-specific humoral and cellular immune responses in mice*. Vaccine 29(34): 5778-84.

Lombard M, Pastoret PP, Moulin AM. (2007). *A brief history of vaccines and vaccination.* Revue Scientifique et Technique (International Office of Epizootics) 26(1):29–48.

Lu, Y. C., Yeh W. C., *et al*. (2008). *LPS/TLR4 signal transduction pathway.* Cytokine 42(2): 145-51.

Luxameechanporn, T., Kirtsreesakul V., *et al.* (2005). *Evaluation of importance of Toll-like receptor 4 in acute Streptococcus pneumoniae sinusitis in mice*. Arch Otolaryngol Head Neck Surg 131(11): 1001-6.

MacLennan IC, Toellner KM, Cunningham AF, *et al*. (2003) *Extrafollicular antibody responses.* Immunol Rev 194:8–18.

Marshall JD, Fearon K, Abbate C, Subramanian S, Yee P, Gregorio J, *et al*. (2003). *Identification of a novel CpG DNA class and motif that optimally stimulate B cell and plasmacytoid dendritic cell functions.* J Leukoc Biol 73(6):781–92.

Medzhitov, R. (2007). *Recognition of microorganisms and activation of the immune response.* Nature 449(7164): 819-26.

Medzhitov, R. (2001). *Toll-like receptors and innate immunity*. Nat Rev Immunol 1(2): 135-45.

Medzhitov, R. and Janeway, C. Jr. (2000). *Innate immune recognition: mechanisms and pathways.* Immunological Reviews 173(1): 89-97.

Mort M, Convery I, Baxter J, Bailey C. (2005). *Psychosocial effects of the 2001 UK foot and mouth disease epidemic in a rural population: qualitative diary based study.* BMJ (Clinical Research Ed) 331(7527):1234.

Müller-Doblies, D., Ackermann M., *et al.* (2002*). In Vitro and In Vivo Detection of Mx Gene Products in Bovine Cells following Stimulation with Alpha/Beta Interferon and Viruses.* Clinical and Diagnostic Laboratory Immunology 9(6): 1192-1199.

Newton, K. and V. M. Dixit (2012). *Signaling in innate immunity and inflammation*. Cold Spring Harb Perspect Biol 4(3).

Neumann AU, Verheij-Hart E, Hellstrand K. (2006). *IP-10 predicts viral response and therapeutic outcome in difficult-to-treat patients with HCV genotype 1 infection*. Hepatology 44 (6): 1617–25.

Nguyen DN, Green JJ, Chan JM, Langer R, Anderson DG. (2009). *Polymeric materials for gene delivery and DNA vaccination.* Adv Mater. 21(8):847–867.

Nierkens, S., M. H. den Brok, *et al.* (2009). *Route of Administration of the TLR9 Agonist CpG Critically Determines the Efficacy of Cancer Immunotherapy in Mice*. PLoS ONE 4(12): e8368.

O'Garra A, Robinson D. (2004) *Development and function of T helper 1 cells.* Adv Immunol 83:133–162.

Pacheco JM, Arzt J, Rodriguez LL. (2008). *Early events in the pathogenesis of foot-and mouth disease in cattle after controlled aerosol exposure.* Veterinary Journal.

Palm, N. W. and Medzhitov R. (2009). *Pattern recognition receptors and control of adaptive immunity*. Immunological Reviews 227(1): 221-233.

Partidos, C. D., Hoebeke J., *et al.* (2009). *Immunomodulatory consequences of ODN CpG-polycation complexes.* Methods 49(4): 328-333.

Rodriguez, L. L. and Grubman M. J. (2009*). Foot and mouth disease virus vaccines.* Vaccine 27 Suppl 4: D90-4.

Samulowitz, U., Weber M., *et al*. (2010). *A novel class of immune-stimulatory CpG oligodeoxynucleotides unifies high potency in type I interferon induction with preferred structural properties.* Oligonucleotides 20(2): 93-101.

Sandgren S., Wittrup A., Cheng F., Jönsson M., Eklund E., Busch S., and Belting M. (*2004) The Human Antimicrobial Peptide LL-37 Transfers Extracellular DNA Plasmid to the Nuclear Compartment of Mammalian Cells via Lipid Rafts and Proteoglycan-dependent Endocytosis* J. Biol. Chem. 279: 17951-17956.

Schmidt M and Olejnik-Schmidt A. (2007) *Biomolecules transfection into animal cells.* Postepy Biochem. 53(4):321-6.

Schröder, M. and Bowie A. G. (2005). *TLR3 in antiviral immunity: key player or bystander?.* Trends in Immunology 26(9): 462-468.

Schwarz K, Storni T, Manolova V, et al. (2003). *Role of Toll-like receptors in costimulating cytotoxic T cell responses.* Eur J Immunol. 33(6):1465–1470.

Seong S, Matzinger P. (2004). *Hydrophobicity: an ancient damage-associated molecular pattern that initiates innate immune responses*. Nature. Rev. Immunol. 4 (6): 469–478.

Sharma S, Tenoever BR, Grandvaux N, Zhou GP, Lin R, Hiscott J. (2003) *Triggering the interferon antiviral response through an IKK-related pathway*. Science 300:1148–51.

Shereck, E., Satwani P., *et al*. (2007). *Human natural killer cells in health and disease.* Pediatr Blood Cancer 49(5): 615-23.

Steinhagen, F., Kinjo T., et al. (2011). *TLR-based immune adjuvants.* Vaccine 29(17): 3341-55.

Sumption K, Rweyemamu M,Wint W. (2008). *Incidence and distribution of foot and mouth disease in Asia, Africa and South America, combining expert opinion official disease information and livestock populations to assist risk assessment.* Transboundary and Emerging Diseases 55(1):5–13.

Stone, K. D., Prussin C., *et al*. (2010). *IgE, mast cells, basophils, and eosinophils.* J Allergy Clin Immunol 125(2 Suppl 2): S73-80.

Sun, E. (2008). *Cell death recognition model for the immune system.* Medical hypotheses 70(3): 585-596.

Takeda K, Akira S. (2005). *Toll-like receptors in innate immunity*. International Immunology, 17(1):1-14.

Takeda, K. and Akira S. (2004). *TLR signaling pathways*. Semin Immunol 16(1): 3-9.

Takeda, K., Tsutsui H., et al. (1998). *Defective NK cell activity and Th1 response in IL-18-deficient mice*. Immunity 8(3): 383-90.

Takeshita F, Leifer CA, Gursel I, Ishii KJ, Takeshita S, Gursel M, Klinman DM. (2001) Cutting edge: Role of Toll-like receptor 9 in CpG DNA-induced activation of human cells. Journal of Immunology, 167(7):3555-8.

Taswell, C. (1981). *Limiting dilution assays for the determination of immunocompetent cell frequencies.* J. Immunol. 126:1614-1619.

Tel, J., A. M. van der Leun, *et al*. (2012). *Harnessing human plasmacytoid dendritic cells as professional APCs*. Cancer Immunol Immunother.

Thoma-Uszynski, S., Stenger S., *et al*. (2001). *Induction of direct antimicrobial activity through mammalian toll-like receptors.* Science 291(5508): 1544-7.

Trinchieri G, Sher A. (2007). *Cooperation of Toll-like receptor signals in innate immune defence*. Nature Review Immunology, 7(3):179-90.

Uhlmann E., Vollmer, J. (2003) *Recent advances in the development of immunostimulatory oligonucleotides*, Curr. Opin. Drug Discov. Dev. 6 204–217.

Valanne, S., J. H. Wang, *et al*. (2011) *The Drosophila Toll signaling pathway*. J Immunol 186(2): 649-56.

Verthelyi, D., Ishii K. J., *et al*. (2001). *Human peripheral blood cells differentially recognize and respond to two distinct CPG motifs.* J Immunol 166(4): 2372-7.

Vollmer, J. R. and Krieg A. M. (2009). *Immunotherapeutic applications of CpG oligodeoxynucleotide TLR9 agonists* Advanced Drug Delivery Reviews 61(3): 195-204.

Vollmer, J. R. (2006). *Editorial: CpG Motifs to Modulate Innate and Adaptive Immune Responses*. International Reviews of Immunology 25(3-4): 125-134.

Vollmer, J., Weeratna R., *et al*. (2004). *Characterization of three CpG oligodeoxynucleotide classes with distinct immunostimulatory activities.* Eur J Immunol 34(1): 251-62.

Wagner, H. (2008). *The sweetness of the DNA backbone drives Toll-like receptor 9.* Curr Opin Immunol 20(4): 396-400.

Waldmann O, Zimmermann T. (1955) *Preparation of foot and mouth disease vaccine according to Waldmann and Kobe using calves as the antigen source.* Zentralblatt fur Bakteriologie, Parasitenkunde, Infektionskrankheiten und Hygiene 1 Abt Medizinisch-hygienische Bakteriologie, Virusforschung und Parasitologie 163(4):239–44.

Walport M., Janeway C., Travers P., and Murphy K.P. (2008). *Janeways Immunobiology*. Garland Science Publishing. pp 823.

Wang G., (2009), Structures of human host defence cathelicidin LL-37 and its smallest antimicrobial peptide KR-12 in lipid micelles. J. Biol. Chem., 283(47), 32637-43.

Wang D, Bhagat L, Yu D, Zhu FG, Tang JX, Kandimalla ER, Agrawal S. (2008) *Oligodeoxyribonucleotide - Based Antagonists for Toll-Like Receptors 7 and 9*. Journal of Medicinal Chemistry.

Watts, C., West M. A., *et al*. (2010). *TLR signalling regulated antigen presentation in dendritic cells*. Curr Opin Immunol 22(1): 124-30.

Weber, F., Wagner. V. (2006). *Double-stranded RNA is produced by positive-strand RNA viruses and DNA viruses but not in detectable amounts by negative-strand RNA viruses.* J Virol 80(10): 5059-64.

Williams R. (2006). *The endosome effect. Journal of Experimental Medicine*. 203(8):1834.

Yamamoto, M., Sato S. (2002). *Cutting edge: a novel Toll/IL-1 receptor domaincontaining adapter that preferentially activates the IFN-beta promoter in the Toll-like receptor signaling*. J Immunol 169(12): 6668-72.

Yamamoto, M., S. Sato. (2003). *TRAM is specifically involved in the Toll-like receptor 4-mediated MyD88-independent signaling pathway*. Nat Immunol 4(11): 1144-50.

Yamamoto M, Sato S, Hemmi H, Hoshino K, Kaisho T, Sanjo H, *et al.* (2003) *Role of adaptor TRIF in the MyD88-independent toll-like receptor signaling pathway.* Science 301:640–3.

Yoon, S.-i., O. Kurnasov, et al.(2012). *Structural Basis of TLR5-Flagellin Recognition and Signaling*. Science **335**(6070): 859-864.

Yoshida, H., Nishikawa M., *et al.* (2009). *TLR9-dependent systemic interferon-beta production by intravenous injection of plasmid DNA/cationic liposome complex in mice.* J Gene Med 11(8): 708-17.

Zhang, L., Zhang J., *et al.* (2011). *Research in advance for FMD novel vaccines*. Virol J 8: 268.

APPENDICIES

A. Buffers, Solutions, Culture Media

Blocking Buffer (ELISA)

- 500 ml 1x PBS
- 25 grams BSA (5%)
- 250 µl Tween20 (0,025%)

Crystal particles of BSA should be dissolved very well, with magnetic-heating stirrer for 20-30 min. The buffer should be stored at -20°C.

Loading Dye (Agarose gel)

- 0,009 grams Bromophenol blue
- 0,009 grams Xylen cyanol
- 2,8 ml ddH_2O
- 1,2 ml 0,5M EDTA
- 11 ml glycerol

After preparing, just vortex it.

PBS (Phosphate Buffered Saline) [10x]

- 80 grams NaCl
- 2 grams KCl
- 8,01 grams $Na_2HPO_4 . 2H_2O$
- 2 grams KH_2PO_4

complete into 1 lt with ddH_2O (pH= 6,8).

For 1X PBS's pH should be ≈ 7,2-7,4 and should be autoclaved prior to use.

PBS-BSA-Na azide (FACs Buffer)

- 500 ml 1x PBS
- 5g BSA (1%)
- 125mg (0,25%)

T-cell Buffer [ELISA]

- 500 ml 1x PBS
- 25 ml FBS (5%)
- 250 µl Tween20 (0,025%)

The buffer should be stored at -20°C.

Wash Buffer [ELISA]

- 500 ml 10x PBS
- 2,5 ml Tween20
- 4,5 lt ddH_2O

RPMI-1640 (Hyclone)

- 2 % : 10 ml FBS (FBS = inactivated at 55°C)
- 5 % : 25 ml FBS
- 10 % : 50 ml FBS
- 5 ml Penicillin/Streptomycin (50 µg/ml final concentration from 10 mg/ml stock)
- 5 ml HEPES (Biological Industries), (10 mM final concentration from 1 M stock)
- 5 ml Na Pyruvate, (0,11 mg/ml final concentration from 100 mM, 11 mg/ml stock)
- 5 ml Non-Essential Amino Acids Solution, (diluted into 1x from 100x concentrate stock)
- 5 ml L-Glutamine, (2 mM final concentration from 200 mM, 29.2 mg/ml stock)

B. Preperation of Complexes

MW of LL-37: 4495 MW of Tat: 1561 MW of K3: 6600

MW of KR-12: 1574 MW of K23: 3960

Table B. Amounts of CpG ODNs and Peptides in complexes

Samples	**Molar ratio**	**K23 (µM)**	**Peptide (µM)**	**K23 (µg)**	**Peptide (µg)**	**K23 (µl) stock 1 λ**	**Peptide (µl) stock 5 λ**	**H2O (µl)**
K23	-	80	-	19.2	-	19.2	-	40.8
K23/LL37	1:1	80	80	19.2	21.54	19.2	4.2	36.6
K23/LL37	1:2	80	160	19.2	43.14	19.2	8.4	32.4
K23/LL37	1:4	80	320	19.2	86.16	19.2	16.8	24
K23/LL37	1:8	80	640	19.2	172.2	19.2	34.2	6.6
K23/KR12	1:2	80	160	19.2	15	19.2	3	37.8
K23/KR12	1:4	80	320	19.2	30	19.2	6	34.8
K23/KR12	1:8	80	640	19.2	60	19.2	12	28.8
K23/KR12	1:16	80	1280	19.2	120	19.2	24	16.8
K23/Tat	1:2	80	160	19.2	15	19.2	3	37.8
K23/Tat	1:4	80	320	19.2	30	19.2	6	34.8
K23/Tat	1:8	80	640	19.2	60	19.2	12	28.8
K23/Tat	1:16	80	1280	19.2	120	19.2	24	16.8

1. To stimulate cells (Volume required for 4 wells): Mix 48.6 µl of complex with 275.4 µl medium and add 50 µl of this to 150 µl cells (for 3 µM ODN dose)

2. Take 75 µl from 3 µM stock (underlined above) and add 150 µl medium; add 50 µl of this to 150 µl cells (for 1 µM ODN dose)

3. Take 22.5 µl from 3 µM stock (underlined above) and add 203 µl medium; add 50 µl of this to 150 µl cells (for 0.3 µM ODN dose).